AN ABSTRACT OF THE THESIS OF

Kurt Thiehsen for the degree of Master of Science in Mechanical Engineering presented on March 17, 1993.

Title: The Effect of Primary Alpha, Nickel, and Chromium on the Creep Properties of Ti 6242Si

Abstract approved: Redacted for Privacy

Michael E. Kassner

Elevated temperature creep tests were performed on Ti 6242Si deformed to small (<0.002) plastic strains using a highly aligned creep testing apparatus. Specimens were solution annealed at various temperatures below the beta transus (T_β -6°C to T_β-52°C) which controlled the volume fraction of primary alpha. Decreases in the amount of primary alpha are associated with decreased primary and steady-state creep rates. The effects of trace levels of the elements Ni and Cr on the creep properties of Ti 6242Si were also studied. Relatively small additions of Ni (0.075-0.093 wt%), which appeared to segregate to the bcc beta phase, substantially increased the creep-rates of this alloy, while additions of Cr up to 0.278 wt% had little, if any, effect on the creep rates.

The Effect of Primary Alpha, Nickel, and Chromium on the Creep Properties of Ti 6242Si

by

Kurt Thiehsen

A THESIS
submitted to
Oregon State University

in partial fulfillment of
the requirements for the
degree of
Master of Science

Completed March 17, 1993
Commencement June 1993

APPROVED:

Redacted for Privacy

Professor of Mechanical Engineering in charge of major

Redacted for Privacy

Chairman of Mechanical Engineering

Redacted for Privacy

Dean of Graduate School

Date of thesis presentation March 17, 1993

Typed by: Kurt Thiehsen

ACKNOWLEDGEMENT

I would like to acknowledge the financial support provided by the U. S. Bureau of Mines, Oregon Metallurgical Corporation (OREMET), and the Oregon Economic Development Department through the Oregon Metals Initiative. I would also like to acknowledge the assistance of Dave Hiatt, Bryan Bristow, Brian Mahoney and Greg Buchanan at OREMET. Finally, I would like to acknowledge the assistance of Utkarsh Kansal with the metallography, and Professor Jun Koike with the TEM in this work.

TABLE OF CONTENTS

LIST OF FIGURES

LIST OF FIGURES (CONTINUED)

LIST OF TABLES

LIST OF APPENDIX FIGURES

LIST OF APPENDIX FIGURES (CONT.)

The Effect of Primary Alpha, Nickel, and Chromium on the Creep Properties of Ti 6242Si

INTRODUCTION

Originally developed in the 1960s for use in high temperature aircraft engine components, the titanium alloy Ti 6Al-2Sn-4Zr-2Mo-0.1Si is classified as a near alpha, alpha-beta alloy. This designation refers to the composition of its microstructure which is composed primarily of an α-phase which has a hexagonal close packed (hcp) crystal structure, although a small quantity of body centered cubic (bcc) β-phase is still present in the microstructure at ambient temperature. The alloy is frequently utilized subsequent to an anneal that is 14°C to 28°C below the beta transus, T_β. The beta transus is the temperature above which only the β-phase is thermodynamically stable in the alloy. A typical microstructure for the alloy when annealed below the β transus consists of equiaxed grains of primary α in a matrix of lenticular α and β platelets. The amount of primary α phase in the microstructure decreases as the solution anneal temperature approaches the β transus.

Ti 6242Si has a combination of light weight, good corrosion resistance, and good creep resistance which makes it a very popular material for jet engine compressor blades. Since it is used primarily for aerospace components in critical areas (i.e. compressor blades) Ti 6242Si must usually satisfy stringent specifications before it is accepted for most applications. A common specification requires an accumulated creep strain of less than 0.001 after 35 hrs, at 241 MPa and 510°C[1]. Creep strain refers to the plastic strain which occurs in a material under a constant stress which is lower than the stress typically associated with macroscopic yielding of the material for a conventional tensile test. There are three stages of creep which are typically observed at elevated temperatures. Stage I or primary creep which begins

when the sample is loaded is characterized by a decreasing creep rate. Stage II creep or steady state creep follows stage I creep and is characterized by a relatively constant creep rate. Stage III creep which follows stage II creep is associated with cavitation in the material and is characterized by continually increasing creep rates until the material fails. Since small strain creep resistance is critical to both in terms of both meeting the aforementioned specification, and the material's performance in various applications, the variables that affect the small plastic-strain creep in this alloy are very important. Thus, this document contains a study of the effects of two variables which can play a major role in creep resistance: the thermal processing of the alloy and the impurity content of the alloy.

REVIEW OF LITERATURE

Ti 6242Si derives its creep strength primarily from the solid solution strengthening provided by its Sn, Zr and Si components all of which are substitutional atoms. The creep properties may be affected by substitutional atoms by changes in threshold stress,[2] elastic moduli, and "atmosphere effects" which refers to viscous drag, dynamic strain aging, or the clustering of solute atoms on dislocations as described by Paton and Mahoney[3]. The creep strength is also very sensitive to microstructure with the finest microstructures generally exhibiting the best creep resistance[4].

Some investigators believe that the controlling creep mechanism at 510°C and 241MPa is Si clustering on mobile dislocations[3,5]. However, others hypothesize that if one accounts for a threshold stress, that creep can be shown to have an activation energy equivalent to that of lattice self diffusion of a Ti thus suggesting a dislocation climb control[2]. Still others believe that the dominant creep mechanism is grain boundary sliding[6].

Work by Bania and Hall[5] indicates that the activation energy for creep (84 Kcal/mol) is higher than that for either self diffusion or silicon diffusion in α Ti at 510°C and 276MPa, but was very close to that reported for "clustering" of Si on mobile dislocations described by Paton and Mahoney[3]. Paton and Mahoney[3] noted that the "clustering" also occurred in titanium alloys similar to Ti 6242Si. They describe the clustering phenomenon as requiring the dislocation to "sweep through the microstructure and collect an Si atmosphere as it moves in order to develop the creep resistant structure rather than for a stationary dislocation to have Si diffuse to it"[3]. They also argue against grain boundary sliding as a rate controlling process by noting that when silicides were formed at grain boundaries (which are expected to inhibit grain boundary sliding) the creep rates were relatively unchanged. They also showed that grain boundary sliding accounted for less than 10% of the creep deformation as

measured by pre and post-creep offset of gold grid lines deposited on the sample by electron beam lithography. Also, by noting that the activation energy for creep was much higher than that for self diffusion or the diffusion of Si in Ti, they indicated that the rate controlling creep mechanism cannot simply be the diffusion of Si in Ti.

Evans and Harrison while studying titanium alloys similar to Ti 6242Si [2] showed that if one accounts for a temperature dependent threshold stress term that the activation energy for creep is in the range of the activation energy for lattice self diffusion or solute diffusion.

Ankem and Seagle[6], however, report that the evidence suggests that for α/β microstructures creep is mainly due to grain boundary sliding. The evidence they present for this argument is that pre and post creep specimens revealed no significant differences in dislocation substructures, and because Si tended to cluster or precipitate on prior β grain boundaries and at α/β interfaces thus inhibiting grain boundary sliding and improving creep resistance.

While there may be some disagreement as to the actual mechanisms of the creep process, investigators have identified several parameters which effect the creep resistance of Ti 6242Si. Previous work by Bania and Hall [5], Seagle et. al. [7], and Chen and Coyne [8] has indicated that the steady-state creep rate may be strongly influenced by the amount of primary α in the alloy and, hence, the solution annealing temperature. This investigation attempted to confirm the steady-state findings of these authors who suggested that by raising the solution annealing temperature toward the β transus, thus reducing the amount of primary α, the steady state creep rate would decrease. Confirming the results was considered important since the data was limited in both quantity and reproducibility. The primary creep range, where previous investigators report inconsistent data, was also investigated in the present study since it dominates the creep deformation at small ($\varepsilon_p<0.002$) creep strains.

Another variable which can dramatically affect the creep properties of Ti 6242Si are small additions of certain alloying elements. For instance, a relatively small quantity of silicon added to the alloy decreases the permanent creep deformation in the alloy after 100 hrs at 510°C and 241MPa from approximately 0.002 at 0.01 wt% Si to 0.0009 at 0.09 wt% Si [7]. Similarly, small amounts bismuth and sulfur added to an alloy similar to Ti 6242Si have been shown increase creep resistance[9]. Conversely, it has also been shown that impurities such as iron [9,6] and oxygen [10] can dramatically degrade the creep properties of the alloy.

It is not uncommon for small concentrations of impurity elements to be present in production ingots of titanium alloys such as Ti 6242Si. Elements such as iron, nickel, and chromium, may leech into the raw sponge during the Kroll sponge production process if stainless steel retorts are used[11]. These elements and carbon can also enter an ingot if recycled titanium chips or machine turnings are used which contain small amounts of other materials such as stainless steel, chipped carbide tooling etc.. The effects of trace levels of nickel and chromium on the creep properties of Ti 6242Si do not appear to have been investigated. Thus, the effects of these two trace elements, were studied because of the importance of the Kroll Process in titanium production.

EXPERIMENTAL PROCEDURE

The samples used for the determination of the effect of the amount of primary a on creep were taken from a production billet of OREMET Ti-6242Si (heat # T 90847) which had a beta transus T_β=1004°C (determined by differential thermal analysis [DTA]). The composition of the billet is listed in Table 1.

The billet was processed by forging a vacuum arc melted 914 mm diameter ingot to a 152 mm diameter billet using a two stage process. The initial reduction was in the beta temperature range between 1065°C and 1149°C (T_β+61 and +145°C) where the ingot was forged to a 254 mm diameter octagon. The final forging at T_β-36°C reduced the diameter to 152 mm . The forged ingot was then cooled to ambient temperature which resulted in a microstructure of principally elongated primary alpha due to relatively slow cooling because of the large diameter of the ingot. Sample coupons were then extracted from the billet and then forged. The samples had initial dimensions of 64 mm x 64 mm x 95 mm. These coupons were heated for 2 hrs. at T_β-36°C +/-14°C before forging. Hammer forging of the samples was performed at OREMET at a strain rate of between 63 s^{-1} and 252 s^{-1}. Six incremental forgings were required to reduce the sample coupon to the desired cross sectional dimensions of 41mm x 16mm. Coupon temperature typically dropped 120°C+/-20°C during each forging increment and the samples were reheated to T_β-36°C +/-14°C after each incremental forging step. The resultant true and engineering strains were 5.1 and 1.81 respectively for the coupon forging sequence. The samples were air cooled after forging and solution annealed at either T_β-6°C, T_β-15°C, T_β-28°C, or T_β-52°C for 1hr, and air cooled. This resulted in lenticular α rather than elongated primary α due to the faster air cooling rate of the smaller samples. The samples were then aged at 643°C for 8 hrs and air cooled to ambient temperature as is consistent with standard practices for this alloy [1]. Tensile samples with a 25.4 mm gage length and a

TABLE I: COMPOSITION OF PRIMARY ALPHA TEST INGOT (wt%)

Al	Sn	Zr	Mo	Si	N	Cr	Ni	Fe	O
6.00	2.02	3.98	2.00	0.08	0.011	0.008	0.005	0.088	0.119

6.35mm diameter were cut from the coupons. The axes of the tensile samples were parallel to the long axis of the forgings.

In order to determine the effects of nickel and chromium on creep, five special 24.4 kg laboratory ingots with small additions of Ni and Cr were prepared by OREMET. The compositions of these ingots appear in Table 2. All of the ingots were forged at the U.S. Bureau of Mines, Albany OR. The 203 mm diameter ingots were heated to 1149°C and soaked for 8 hours then forged to 165 mm octagons in 3 steps with a 20 minute reheat to 1149°C between each forging step. Then the sample was air cooled until the metal visually appeared to be at ambient temperature and subsequently reheated to 945°C for 90 minutes. The ingot was then forged in two steps down to a 127 mm square with a 20 minute reheat to 945°C (below T_β) between the steps. Next, it was beta annealed at 1038°C for 80 minutes and water quenched. Following quenching, the ingot was reheated to 971°C for 90 minutes and then forged in 9 steps down to a 57 mm square with a 20 minute reheat to 971°C after each step. Sample coupons were then extracted from the billet and hammer forged using the same procedure used to make the samples for determining the effect of primary α except that all coupons were solution annealed at T_β-15°C

Figure 1 shows part of testing system used in this investigation. All of the creep tests in this study were performed on a modified Arcweld (SATEC) model UC creep testing machine. The modifications to the machine were performed because significant anomalies including variations in elastic strain on loading of up to 285% and poor reproducibility of the creep-rates were observed in data taken during preliminary tests. These anomalies had several potential sources including extensometer slippage, inconsistent sample properties, or bending in the sample due from the creep testing machine. Visual and micrographic inspection of test samples indicated that the samples had homogeneous microstructures, were of consistent dimensions, and high quality. A series of repeated unloadings and reloadings

TABLE II. NICKEL AND CHROMIUM TEST INGOT COMPOSITIONS (wt%)

Ingot #	Cr	Ni	Fe	Al	Sn	Zr	Mo	O
0	0.005	0.010	0.076	5.75	2.26	3.77	2.00	0.140
1	0.007	0.093	0.076	5.90	2.30	4.00	2.00	0.158
2	0.008	0.075	0.080	5.95	2.43	4.18	2.00	0.148
3	0.071	0.011	0.074	5.84	2.38	4.11	1.93	0.131
4	0.270	0.011	0.064	5.85	2.38	4.23	1.93	0.127

Figure 1. Creep Testing System

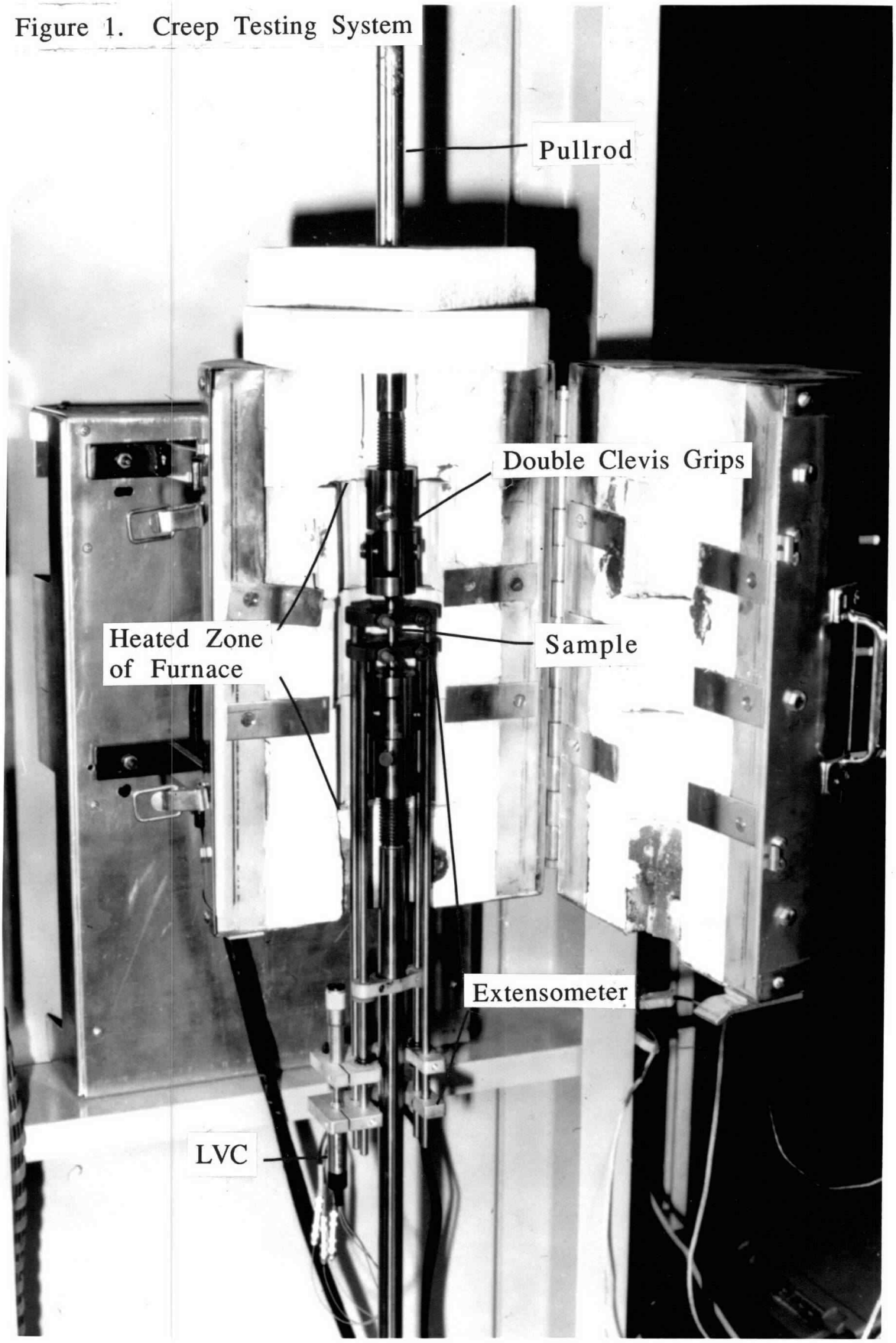

of a single sample showed that for a fixed orientation of the sample in the grips the repeatability of the elastic strain on loading was +/-2%. This indicated that extensometer slippage or hysteresis in the extensometer was not a significant concern. Checking for bending using a sample equipped with four strain gages mounted at 90° intervals around the gage section, it was determined that bending moments were being imposed on the sample by the testing system. This was a significant concern because using an extensometer equipped only with a single linear variable capacitance transducer (LVC-a strain measuring device), strain on only one side of the sample could be determined and bending moments in the sample were impossible to detect directly. The level of bending observed would be insignificant in a conventional (e.g. 0.1-0.2 plastic strain) creep test . However, at the very low plastic strains measured in this investigation (<0.002) and the relatively high elastic strain on loading (~0.0035), less than perfectly aligned testing systems can have bending moments that cause a stress gradient. Stress gradients can cause anomalously high or low creep rates as measured by a single extensometer. To ensure minimal bending, creep test machine pull rods, precision ground straight to within 0.01 mm, using stress relieved Inconel 600 were utilized. High-temperature double clevis universal-type specimen grips were designed and fabricated from X750 Inconel. Another universal was added to the lower part of the standard "load train". Thus, a total of four universal joints were present in the load train. The universal grips were lubricated with graphite.

Sample stress was calibrated using an Instron load cell mounted in the load train. The stress was measured on the front panel of an Instron 4505 test frame. Weights were added to the creep tester load pan until the calculated stress in the sample was 241 MPa +/-4MPa (the limit of the accuracy of the load cell).

During testing it was also noted that there was some fluctuations in the data which appeared to be related to ambient temperature fluctuations in the room. Because the fluctuations

reduced the quality of the data, an insulated enclosure was built to protect the LVC and external extensometer elements. Both the LVC and the lower third of the extensometer were located on the exterior of the apparatus and thus subject to variation in ambient temperature, humidity, drafts etc. during the course of the 72 hours the creep tests typically ran. This enclosure appeared to significantly improve the data quality although the LVC temperature still varied by as much as +/-5°C.

The standard recommended practices for determining the magnitude of bending were utilized prior to all creep tests [12,13]. It was determined that Ti 6242Si did not measurably creep at ambient temperature at 241 MPa (the standard applied creep stress). This allowed strain gages to be mounted on all creep test samples for ambient temperature pre-alignment at 241 MPa . Four strain gages were mounted at 90° intervals around the sample, and the bending in the sample was then measured for various orientations of the sample within the threaded universal grips. A configuration that minimized the bending at ambient temperature was identified. Bending values were calculated according to the following formula:

$$\%\ \text{bending} = \frac{((\text{average strain})-(\text{max. or min. strain}))\times 100}{(\text{average strain})} \qquad (1)$$

The improvements to the apparatus allowed a reduction of test sample bending at ambient temperature to less than 4% (and as low as 0.7%). The strain gages were then removed while the sample was still loaded to prevent misalignment during stripping. The adhesive was removed, and the sample was then given a final cleaning with methanol. Three thermocouples were attached, at the top, middle, and bottom sections of the specimen gage length. This allowed for precise temperature monitoring and control. The extensometer was then attached to the sample which was then unloaded to 25MPa (a stress at which no measurable creep occurs

at 510°C) and heated to 510°C. The creep tests were commenced once the temperature was allowed to stabilize at 510°C +/-2°C for 3.5-4.5 hours. A three zone furnace with Eurotherm power supplies and controllers was utilized. The samples were tested for 72 hours (or longer) to ensure that a mechanical steady-state was achieved. The temperature typically did not vary by more than two degrees from 510°C at any point along the specimen throughout the test. All creep data reported in this thesis are unaltered raw data; "smoothing" was not performed. The creep strain was measured using a single Applied Test Systems model 4112 extensometer configured for 6.35mm dia. samples with 25.4mm gage lengths, and a Measuretron model L1-12 linear variable capacitance transducer. The extensometer was determined to have an error of less than +/- 50 microstrain over a 72 hr period. Thermocouple and raw strain data were taken and digitized using a Fluke 2620A data acquisition unit which fed the data via an IEEE 488 GPIB interface to an Apple Macintosh computer. Computer data manipulation was done using Labview and Cricket Graph.

After creep testing, the samples were sectioned and the microstructures were examined by optical metallography, and transmission electron microscopy (TEM).

The optical metallography was performed as follows: Metallographic sections were taken parallel and perpendicular to the tensile axis. Two parallel sections were extracted that were 90° apart using a low speed saw with a silicon-carbide (SiC) abrasive blade. The samples were then ground successively on 240, 320, 400, and 600 grit SiC paper and subsequently polished using 5, 0.3, and 0.05μm alumina powder slurries. The samples were then etched using a solution of 10 ml HF, 15 ml HNO3, and 75 ml water. Area fractions of primary α were determined using by taking the video camera output from an Olympus PME optical microscope into a Macintosh II computer and analyzing the data using Automatix Inc.'s image analyzer version 7.2. The analysis of

the metallographic specimens was verified by manual point counting method.

The TEM foils were produced from 0.5mm sections extracted from the gage section that were perpendicular to the tensile axis using a low speed diamond cutting saw. These were ground to a thickness of 150 μm in stages using 30μm, 12μm, and 3μm alumina polishing paper. 3mm diameter disks were subsequently cut from the center of the slices by an abrasive slurry disk cutter. The disks were then jet polished at -40°C to perforation using a solution consisting of 10% $HClO_4$, 10% isobutyl alcohol, 80% methanol at 25 V. The microstructure was examined with a Phillips CM12 scanning transmission electron microscope (STEM) operated at 120 kV. Composition analysis was performed using a Kevex X-ray energy dispersive spectrometer (XEDS) attached to the STEM with an electron beam size reduced to ~10nm.

RESULTS

A. Effect of Primary α-phase

Figure 2a-d shows the typical microstructure of hammer forged samples solution annealed at T_β-6°C, T_β-15°C, T_β-36°C, and T_β-52°C. Bands of elongated primary alpha are evident at lower annealing temperatures but diminish with higher solution annealing temperatures. A companion study suggests that the elongated primary alpha grains observed in the samples solution annealed at or below 1018°C may be remnants of the elongated alpha of the forged billets [14].

The dependence of the amount of primary α on solution annealing temperature (relative to the beta transus) is shown in Figure 3. As anticipated, the amount of primary α in the sample is a strong function of the solution annealing temperature. With the exception of the T_β-6°C samples which contained slightly less primary α than predicted, the percentages of primary α all fall within the ranges reported by Seagle et. al.[7]. However, the fractions were generally higher than those predicted by Bania and Hall (who determined the T_β micrographically rather than by DTA)[5]. Some scatter is evident in the data, particularly at higher percentages of primary α.

Figure 4a shows a summary of the primary creep strain as a function of volume fraction of primary α (the individual creep curves for all of the tests performed can be found in the appendix). The onset of stage II creep typically occurred at a plastic strain of 10^{-3}. Figure 4b shows a summary of the dependence of the steady-state (stage II) creep-rate on the volume fraction of primary α. It is apparent that the steady state creep rate varies inversely with the volume fraction of primary α. Since bending stresses decrease with plastic strain, the stage II or steady state creep value may be the most reliable indicator of creep resistance. The scatter bands appear significant, however, the "average scatter" was biased by an anomalously low creep rate for one of

Figure 2. Optical Micrographs of Samples annealed at:
a) T_β-6°C, b) T_β-15°C, c) T_β-28°C, and d) T_β-52°C

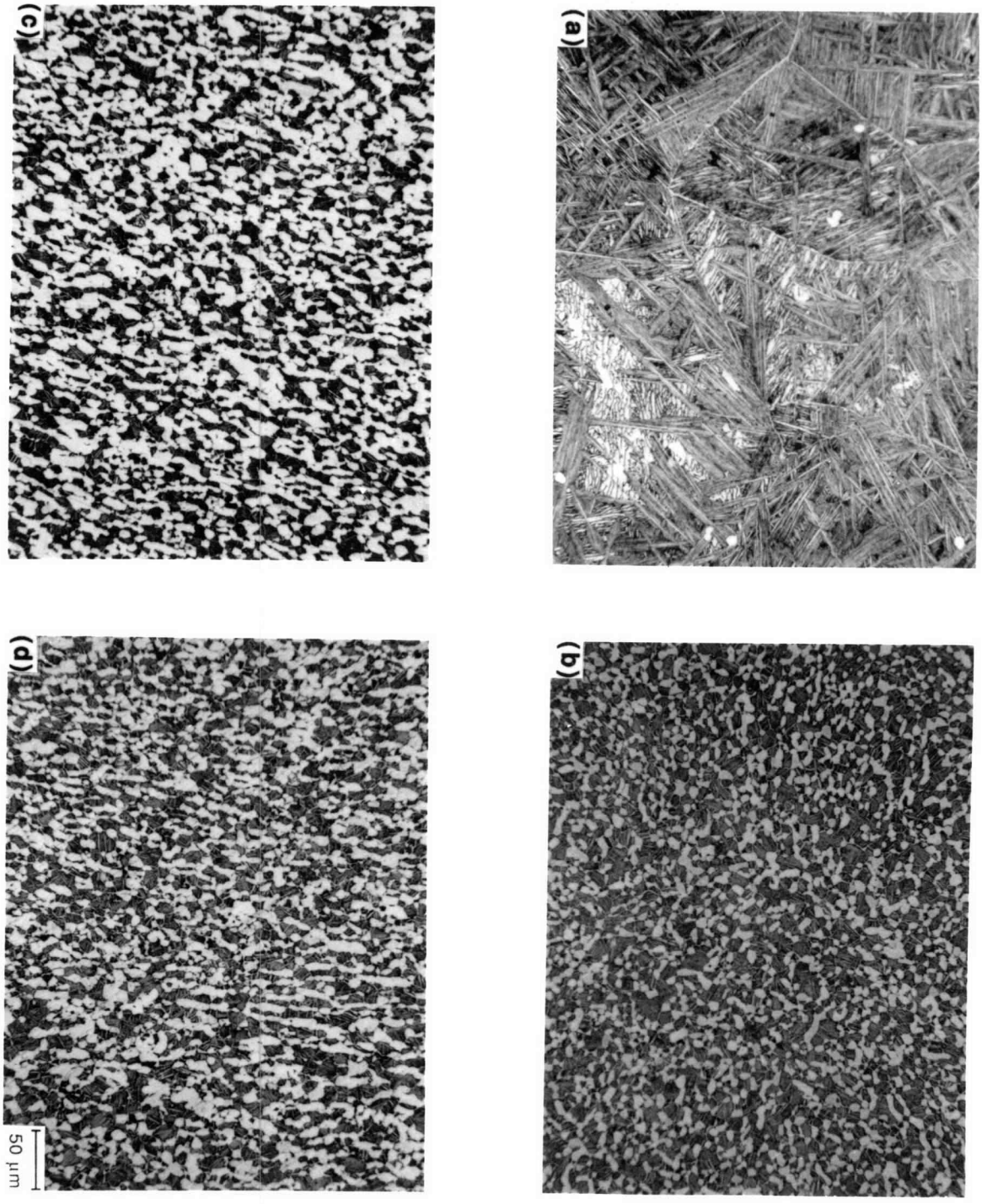

Figure 3. The Effect of Solution Annealing Temperature on Primary Alpha

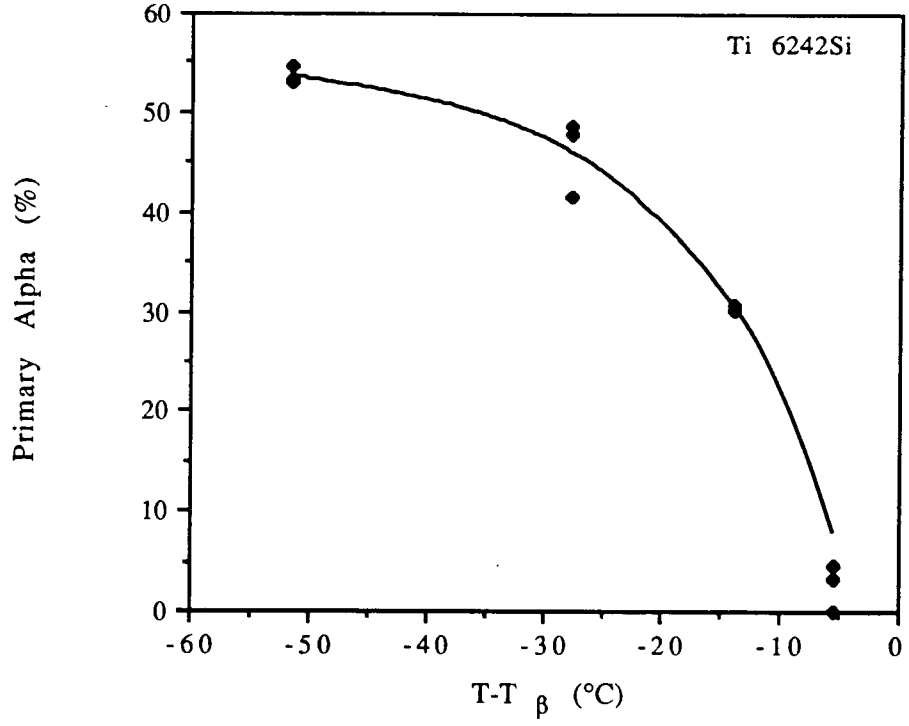

Figure 4. The Effect of Primary Alpha on Creep Deformation

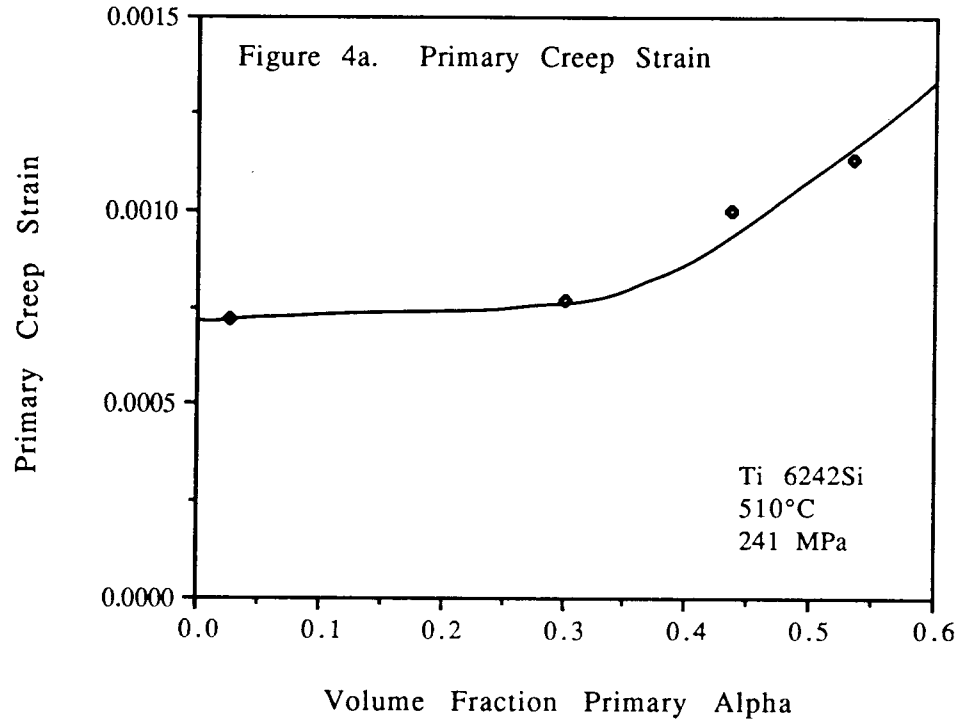

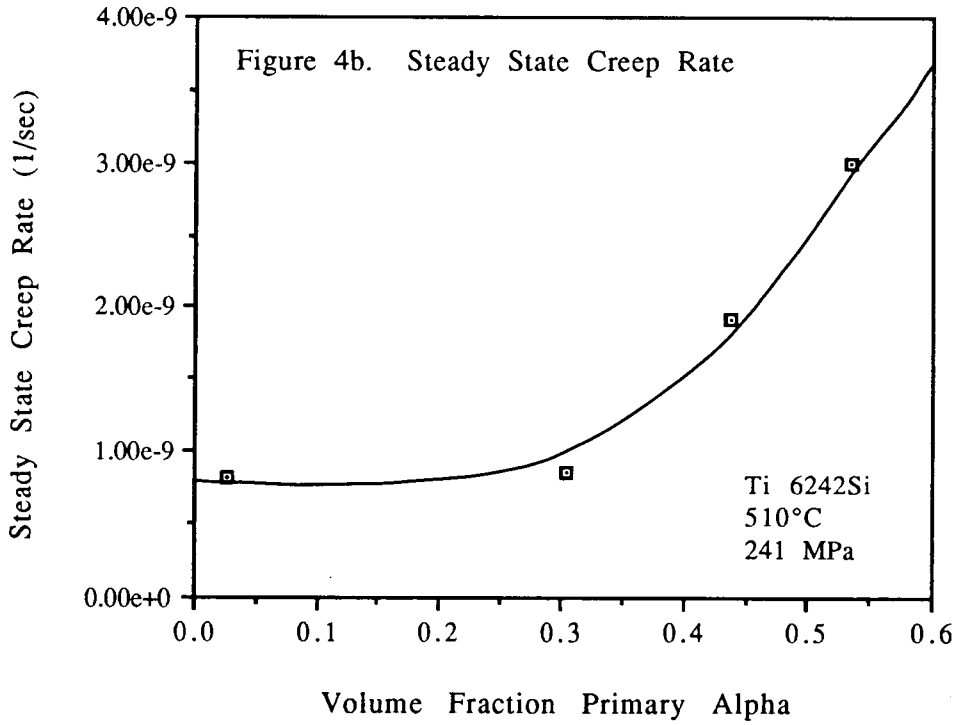

the three tests at the lowest fraction of primary α. The data are reported as an average of three tests at each primary α percentages corresponding to their respective solution annealing temperature as found in Figure 3.

Figure 5 shows a typical creep curve for Ti 6242Si solution treated at T_β-15°C, note that well defined primary and steady-state creep regimes are present.

It was also observed that the room temperature elastic modulus dropped slightly with an increase in the amount of primary alpha as shown in Table III.

B. The effects of Ni and Cr

Figure 6 compares the creep-rate curves of two Ti 6242Si specimens solution treated at the same temperature (T_β-14°C) containing 0.01 and 0.093 wt% Ni (all of the original curves generated can be found in the appendix). It is obvious that small additions of Ni can dramatically degrade the primary and steady-state creep resistance of Ti 6242Si. The summary of the effects of Ni on the primary and steady-state creep rates are shown in figures 7a and 7b. Based on the slope of the best fit line through the steady state creep data in Figure 6b, Ni may increase the steady state creep rate by about 8000% per wt% Ni over the range of Ni concentrations from 0.01 wt% to 0.1wt%. Similarly, figure 6a shows that the primary creep also increases by approximately 5000% per wt% Ni over the range of Ni concentrations studied. Examination of the sample with the highest Ni concentration (0.093 wt%) by optical metallography and TEM showed the microstructure to be typical for this alloy for the heat treating conditions used. Figures 8a and 8b show TEM micrographs of α and β platelets. No nickel rich precipitates were observed although fine interfacial a was noted at the α/β interfaces as expected [5]. The β phase is quite thin at only about 10-25nm. The results of a XEDS analysis are shown in Table 3. It appeared that all of the Ni and the Fe (also known to degrade creep resistance [6]) segregated to the β phase. In addition to the

Table III: ROOM TEMPERATURE ELASTIC MODULI OF Ti 6242Si

Primary Alpha (%)	Elastic Modulus(strain gage)
3%	118 GPa
31%	116 GPa
43%	115 GPa
54%	114 GPa

Figure 5. Typical Creep Curve For Ti 6242Si

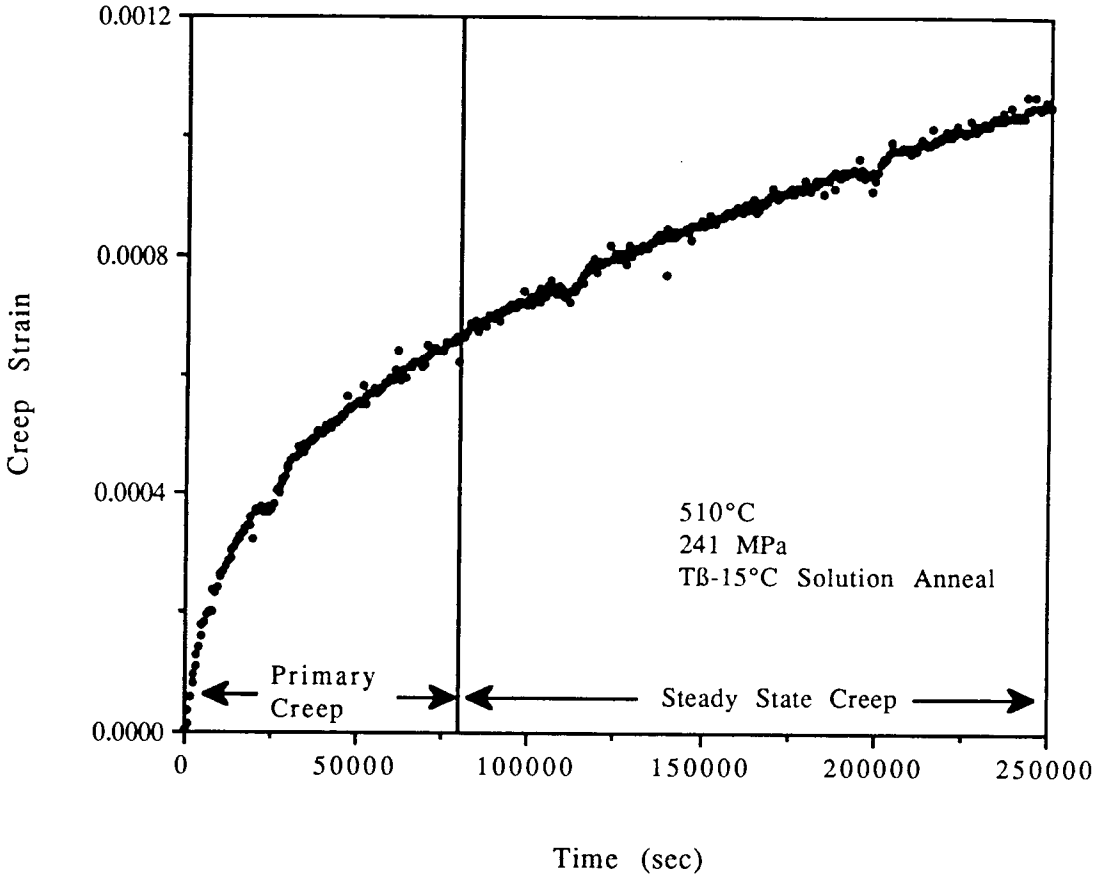

Figure 6. Comparison of Creep Curves for Ti 6242Si with Additions of 0.01 and 0.093 wt% Nickel

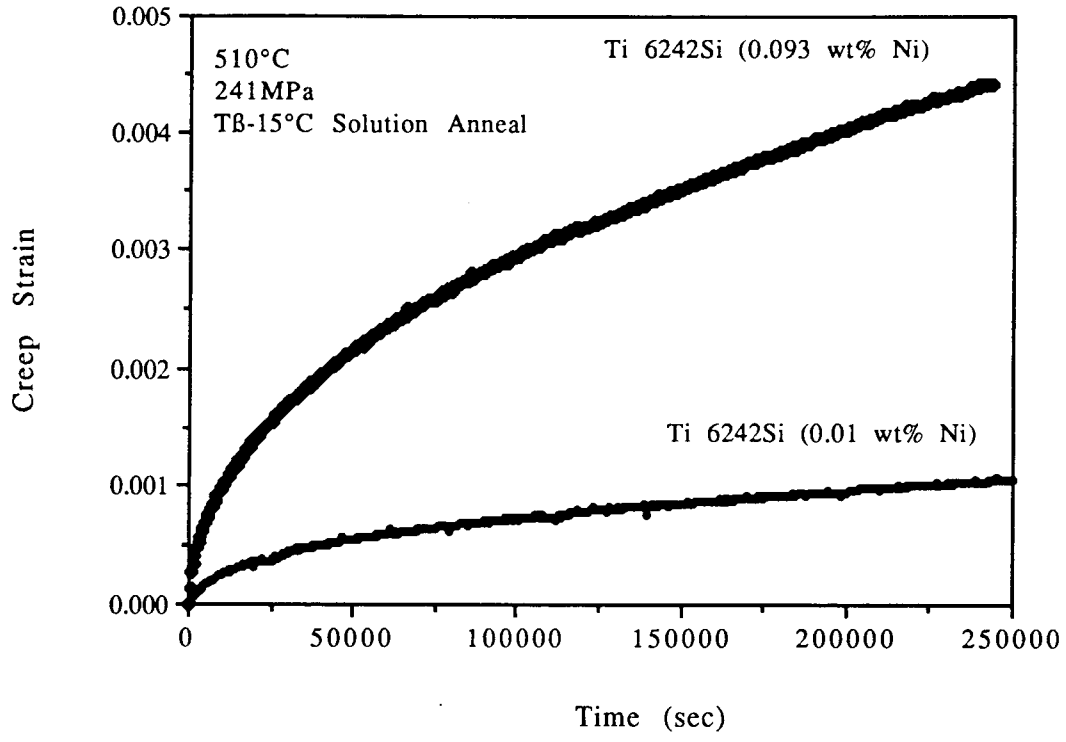

Figure 7. The Effect of Nickel on Creep Deformation

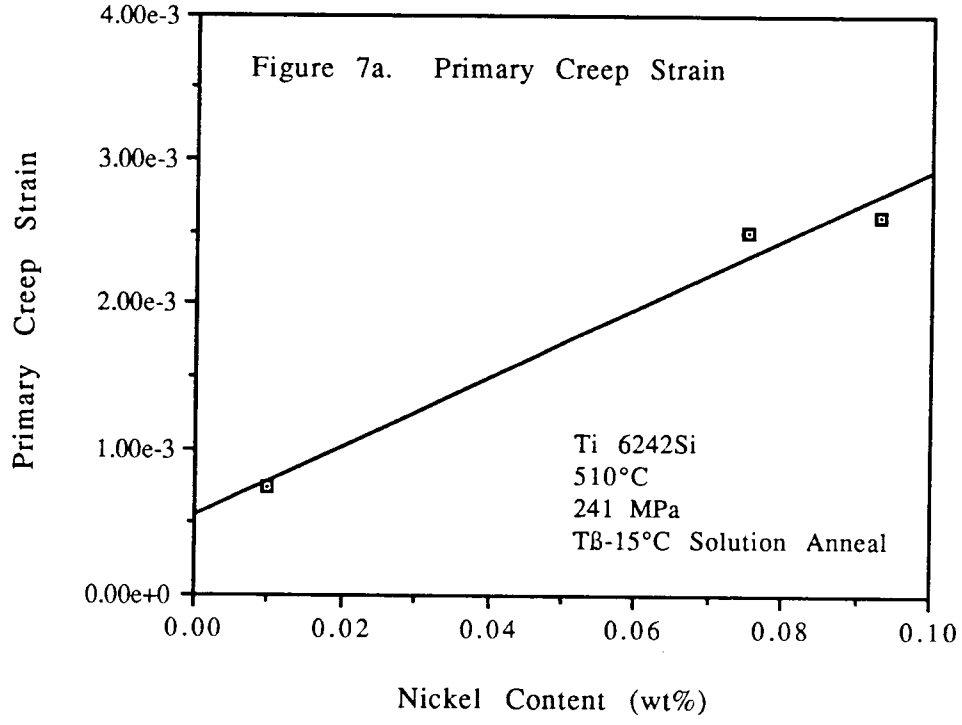

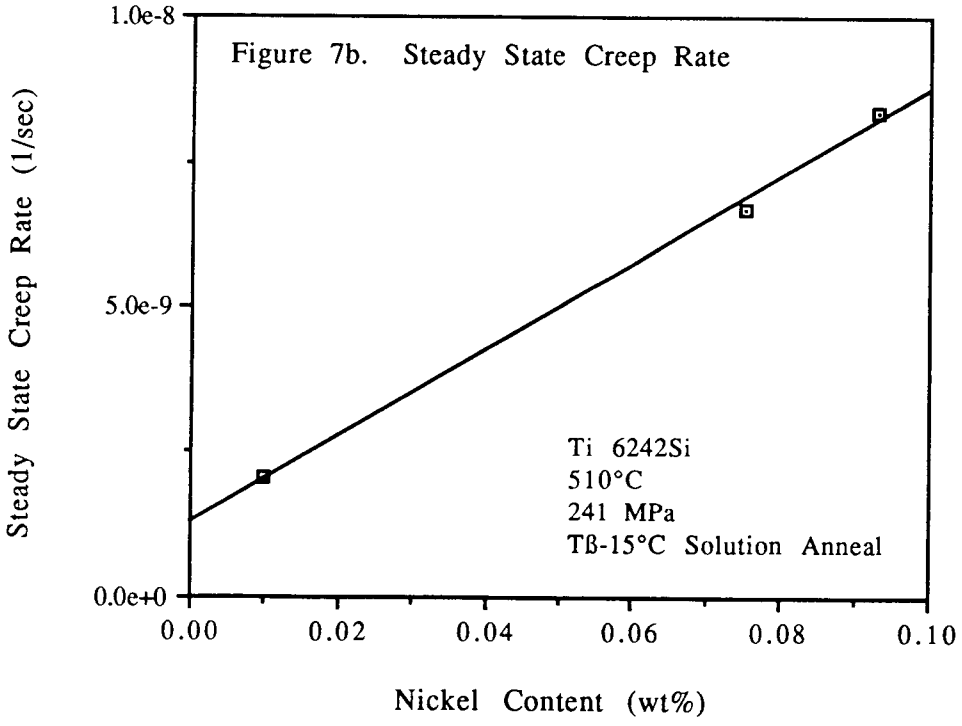

Figure 8. STEM Micrographs of Creep Tested Ti 6242Si

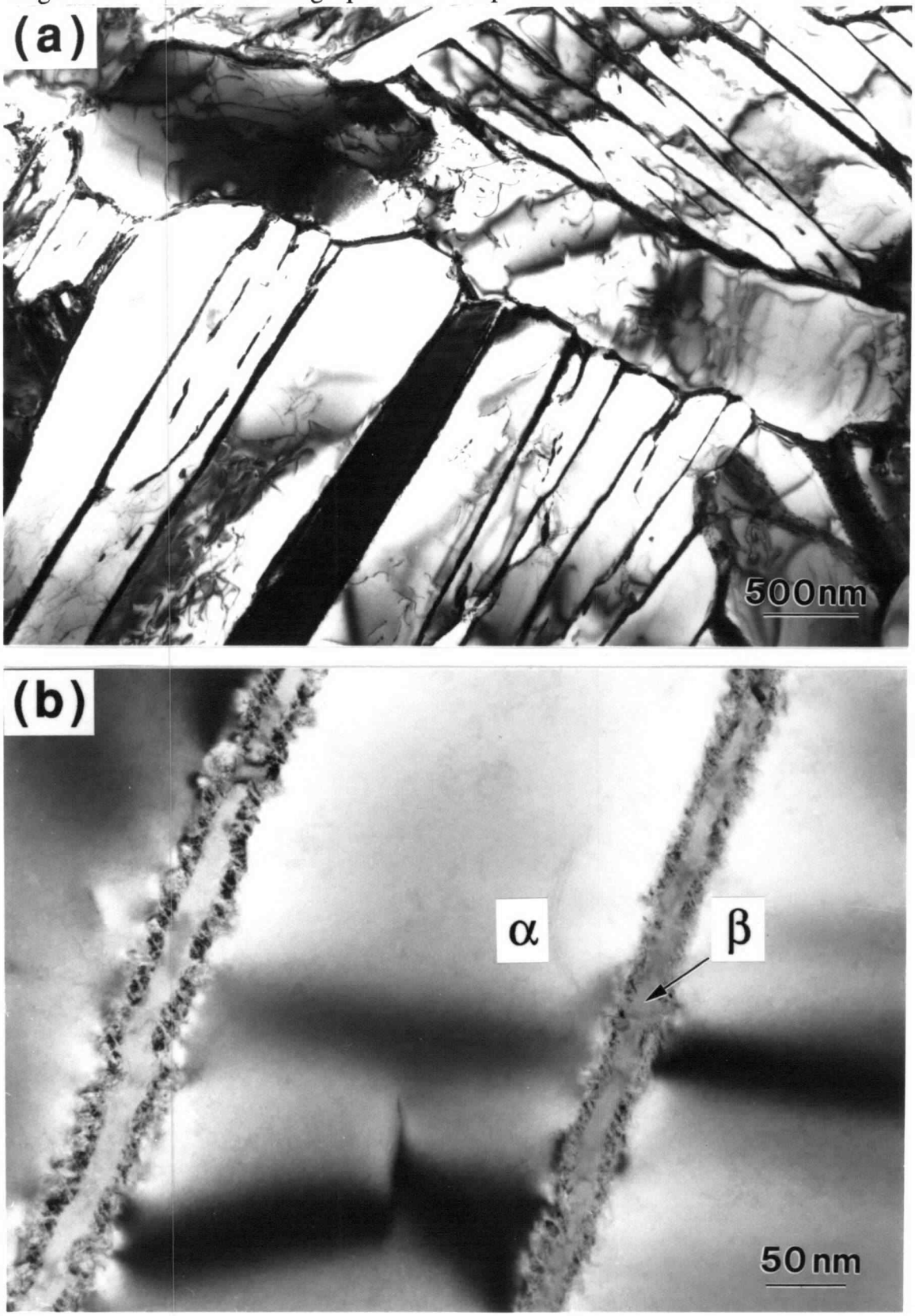

segregation of Ni and Fe, Sn appears to somewhat segregate to the α phase . The anomalously high oxygen content determined by XEDS is probably due to surface oxidation after jet polishing. The effects of Cr on the creep properties are reported in Figures 9a and 9b. It appears that Cr has little, if any, effect on the creep properties of Ti 6242Si.

Finally, it should be noted that in all of the creep tests performed (both for determining the effect of primary α and for the Ni and Cr impurity tests) an anelastic recovery of some of the plastic strain (typically ~0.0006) occurred. An example of the typical anelastic recovery observed in our tests is shown in figure 10.

TABLE IV. COMPOSITIONS OF α AND β PHASES IN Ti 6242Si (WITH 0.93 wt% NICKEL) DETERMINED BY XEDS (wt%)

INTERIOR α PHASE

Element:	O	Al	Si	Ti	Cr	Fe	Ni	Zr	Mo	Sn
Quantity:	2.87	5.51	0.38	85.24	0.33	0.00	0.00	2.75	0.49	2.15
St. Dev.:	0.86	0.70	0.18	3.92	0.25	0.00	0.00	0.76	0.33	0.75

INTERFACIAL α PHASE

Element:	O	Al	Si	Ti	Cr	Fe	Ni	Zr	Mo	Sn
Quantity:	2.04	4.97	0.12	90.25	0.05	0.00	0.00	1.66	0.00	0.85
St. Dev.:	0.73	0.66	0.10	3.94	0.09	0.00	0.00	0.59	0.00	0.47

INTERIOR β PHASE

Element:	O	Al	Si	Ti	Cr	Fe	Ni	Zr	Mo	Sn
Quantity:	4.40	4.78	0.23	85.53	0.13	0.43	0.33	2.55	0.31	0.74
St. Dev.:	1.04	0.63	0.13	3.82	0.15	0.30	0.30	0.71	0.14	0.43

Figure 9. The Effect of Chromium on Creep Deformation

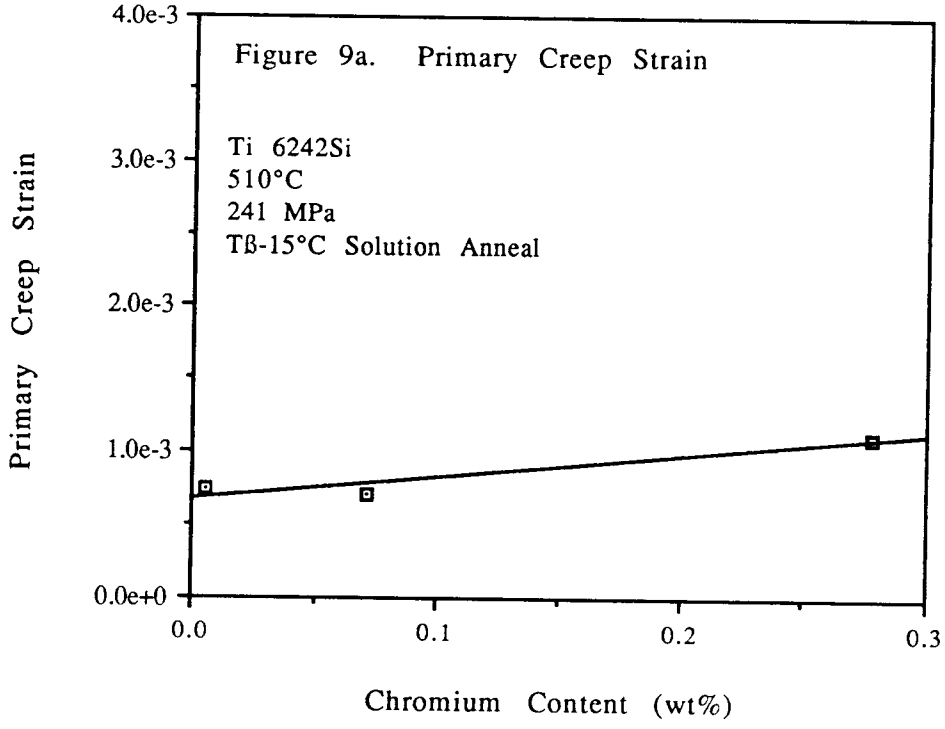

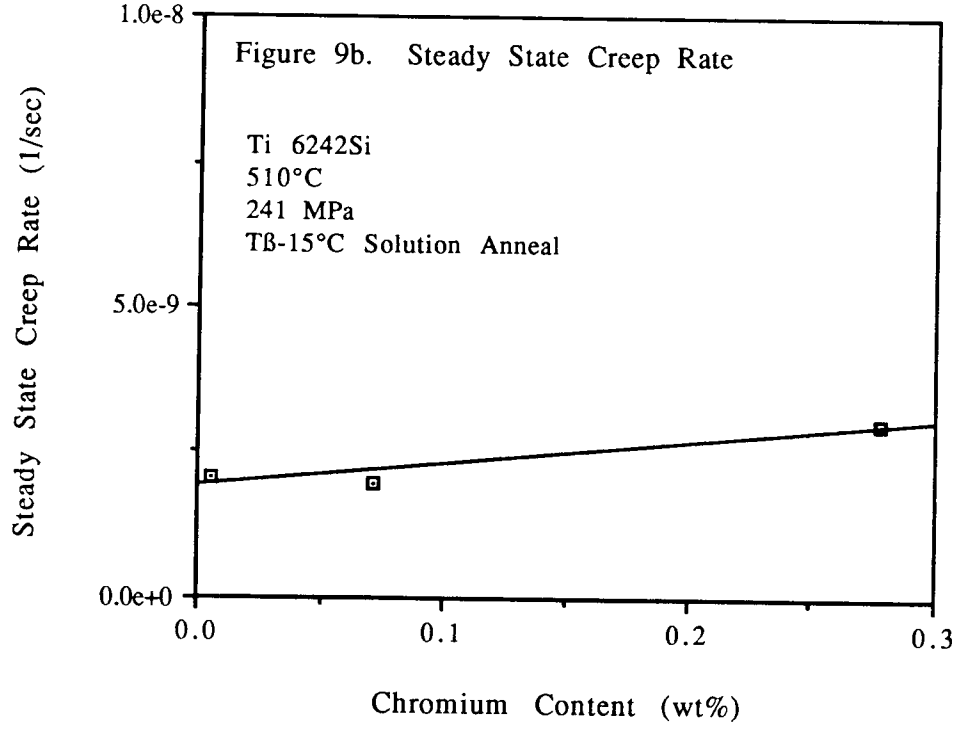

Figure 10. Typical Anelastic Recovery of Plastic Strain (Ti 6242-0.1Si Tß-19°C solution anneal)

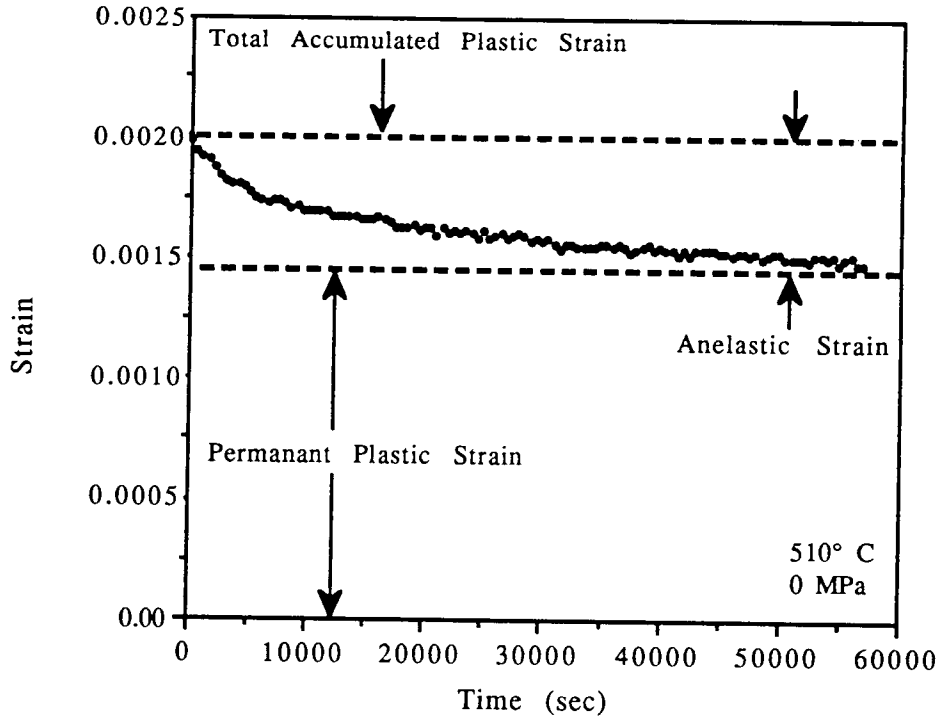

DISCUSSION

As mentioned in the review of literature, the basic mechanism of Ti 6242Si creep at the temperature and stress used in this investigation is not well understood. Thus, it is difficult to explain the trends in terms of a basic mechanism. However, the observed increase in steady state creep rate with increasing amounts of primary α was expected based on the work of Bania and Hall [5], Chen and Coyne [8], and Seagle et. al. [7]. Chen and Coyne [8] reported approximately a threefold increase in the time to 0.002 total creep strain for $\alpha+\beta$ forgings as the solution annealing temperature is raised from T_β-45°C to the beta transus (at 566°C and 211MPa). Seagle et. al. [7] reported an approximate 40% increase in total creep deformation as the solution annealing temperature was lowered from T_β-12°C to T_β-42°C. Bania and Hall [5] found that a decrease in primary α from 35% to 0% resulted in a threefold decrease in steady state creep rate, while the effects on primary creep were unclear.

In this study, a decrease in steady-state creep rate of approximately fivefold upon reducing the amount of primary alpha from 53% to 3% or a threefold decrease in creep rate with a reduction of primary α from 35% to 0% was observed, which appears consistent with earlier findings[5]. The work presented here is important since it confirms the earlier steady-state trends, but more significantly, primary creep trends are established.

One possible explanation for the observed α-phase trends would be that the decrease in creep rate may be due to a more refined microstructure with less primary α. It has also been established that smaller grain sizes (a more refined microstructure) may result in greater creep resistance [15]. Semiatin and Lahoti [16] suggested that both texturing and banding can as much as double the observed creep strain. Based on the observed banding in our specimens annealed at lower temperatures, texturing may be more pronounced at lower

annealing temperatures (larger fractions of primary α), thus leading to higher creep rates. In as much as the β-phase is important with respect to small-strain creep, as will be discussed subsequently, the change in solution annealing temperature may affect the β-phase morphology and thus the creep-rate. Thus the "effect" of primary a on the creep properties may be artificial or indirect.

Another possible explanation for the decrease in primary and steady state creep rate with increasing is that the elastic modulus decreases with increasing amounts of primary alpha see Table III. Sherby and Burke [17] proposed the classical empirical relation for strain rate (for 5-power-law creep):

$$\text{Strain Rate} = AD_0 \exp(-Q/RT)(\sigma/E)^n (\gamma^{3.5}/L^2) \qquad (2)$$

D_0= diffusion constant, Q= activation energy of diffusion, σ= applied stress, E= elastic modulus, γ = stacking fault energy, A= constant, n= constant (4 to 5 above 0.6 T_m), R= gas constant, T= absolute temperature, L= grain size.

Assuming the relative difference between elastic modulus and and primary alpha persists at 510°C, then, using the preceding equation and the data from Table II, we would predict that the steady state creep rate for the T_β-6°C solution annealed samples would be 14% less than that of the T_β-52°C solution annealed samples. This difference, however would only explain part of the observed trend, although the entire difference might be explained in terms of smaller grain sizes.

While Ti 6242Si is a very complex alloy (six primary constituent elements, several common impurity elements, and an hcp α phase with a bcc β phase) much of the previous research has treated the alloy as essentially a homogeneous material in terms of determining creep mechanisms. This approach may be too simplistic to accurately characterize the creep phenomenon and perhaps the material should be viewed as a composite instead.

Since Fe [2,10] and Ni, which we find dramatically degrade the creep properties appear to segregate exclusively to the beta phase, creep in this phase may be the dominating factor in this alloy at 510°C and 241 MPa at least over the small strain range examined. This may also be consistent with the fact that steady-state is observed in the "bulk" (90% α-phase) after only 0.001 strain. In reality, the strain in the β phase may be much higher and is thus more consistent with the values of strain typically observed for the onset of steady-state creep [17]. One theory suggests that Fe may interact with Si (present in both the α and β phases) in such a way that it reduces the ability of Si to inhibit plasticity[6]. This theory might also apply to Ni . Also, since it appears that the Ni and Fe segregated (in solution) to the β phase, it is possible that they could enhance self diffusivity in the bulk β phase or at the grain boundaries thus assisting climb-controlled creep or grain boundary sliding. This is speculative since no data is currently available as to the effects of Fe and Ni on the self-diffusion of the β phase in Ti 6242Si.

A major focus of this work was the development of an equation to predict the creep strain in Ti 6242Si at the test conditions typically used for qualification of the alloy for use in aircraft engines (less than 0.001 strain at 510°C 241MPa after 35 hours). Based on statistical analysis of the data obtained in this study and the data gathered by Ankem and Seagle[6] on the effects of iron on creep in Ti 6242Si, empirical relations have been obtained to predict these creep properties as a function of Ni and Fe content and primary α content in the alloy. The predictive equation for creep strain at 35 hrs is:

$$\text{Creep Strain} = -144\times10^{-6}+0.0240(W_n)+0.0085(W_f) -556\times10^{-6}(V_\alpha)+261\times10^{-5}(V_\alpha)^2 \qquad (3)$$

Where W_n is the weight percent Ni W_f is the weight percent Fe, and V_α is the volume fraction of primary a phase. Note that while it is believed that the equations will yield reasonable predictions

of creep properties other processing parameters such as cooling rates from forging, the presence of impurities other than Ni and Fe, or variations in alloy composition may reduce the quality of the equation's predictions. Figure 11a shows the predicted creep for a sample containing 0.088 wt% Fe and 0.005 wt% Ni as a function of primary α volume fraction. Figure 11b shows the predicted creep for a sample containing 30% primary α and 0.088 wt% Fe as function nickel content. Finally, figure 11c shows the predicted creep for a sample containing 30% primary α and 0.005 wt% Ni as a function of iron content.

Figure 11. Estimated 35 hour Creep Strain

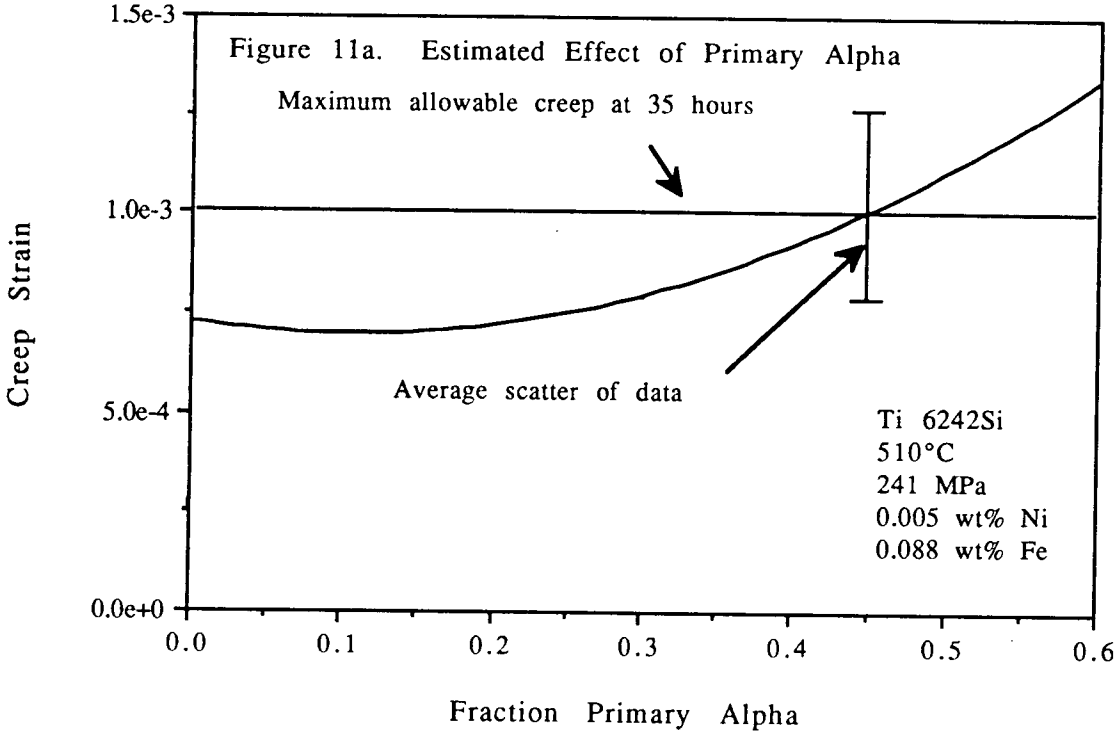

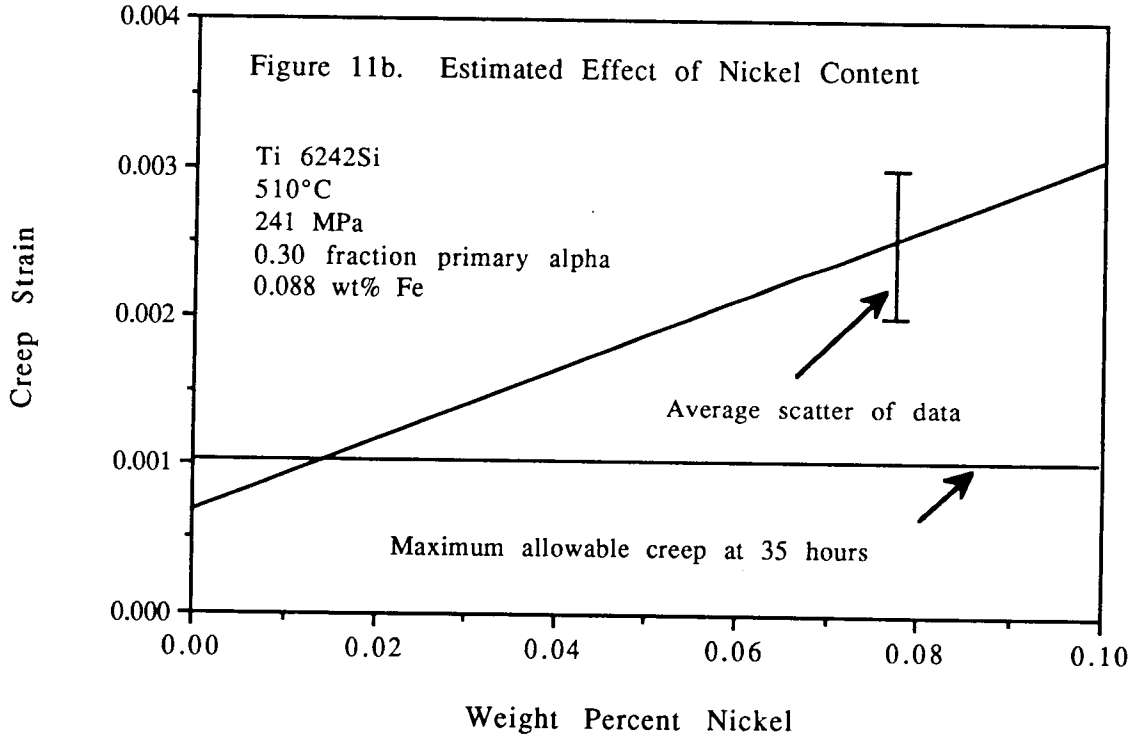

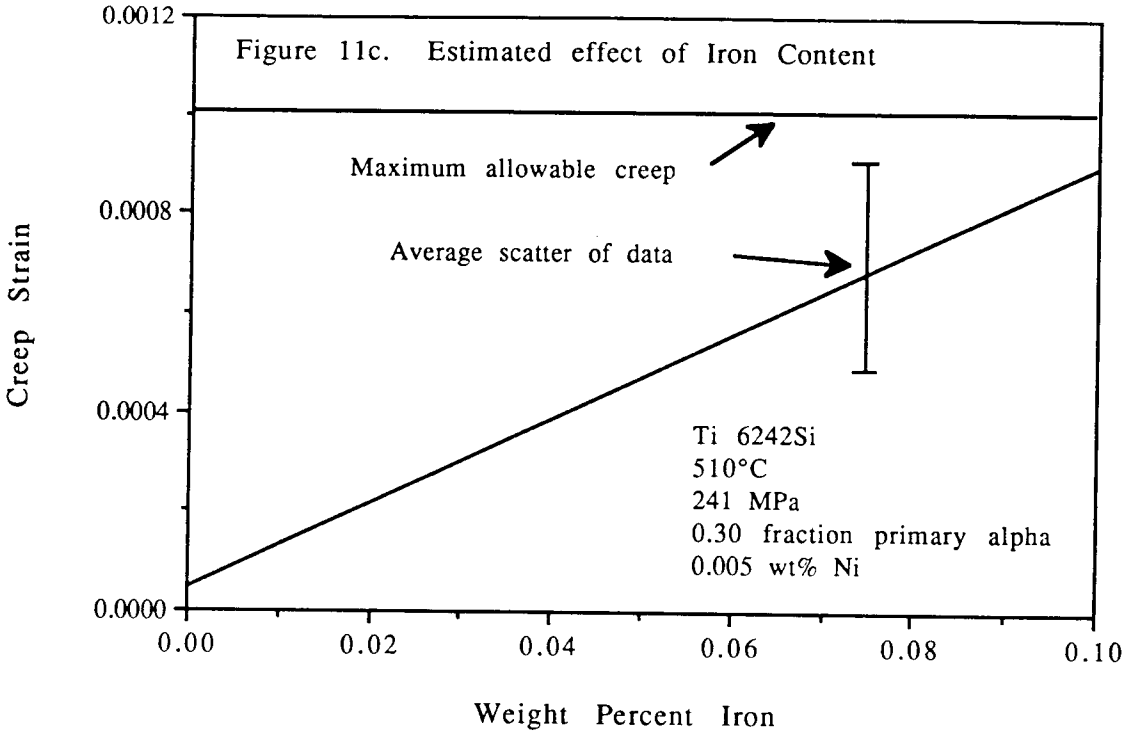
Figure 11c. Estimated effect of Iron Content
Maximum allowable creep
Average scatter of data
Ti 6242Si
510°C
241 MPa
0.30 fraction primary alpha
0.005 wt% Ni
Creep Strain
0.0012
0.0008
0.0004
0.0000
0.00
0.02
0.04
0.06
0.08
0.10
Weight Percent Iron

CONCLUSIONS

1) Improved testing procedures show that raising the solution annealing temperature appears to increase both the primary and steady state creep resistance of Ti 6242Si. This beneficial effect may be derived from a combination of several sources including the removal of such micrographic features such as banding or texturing, and especially the altering or refining of the α or β microstructure.

2) Small concentrations of Ni appear to segregate uniformly into the β phase and dramatically degrade the creep properties of Ti 6242Si. The explanation for this is unclear.

3) Small additions of Cr have little, if any, effect on the creep resistance of the alloy.

4) The β phase, which comprises only about 10% of the alloy may have a much more important role in the creep of Ti 6242Si over the small strain-range examined than previously acknowledged.

5) An equation can be formulated to reasonably predict the creep strain after 35 hours at 510°C and 241 MPa in terms of primary α, Ni, and Fe content. This relationship is valuable in assessing the probability of a Ti 6242Si sample meeting industry qualification specifications.

BIBLIOGRAPHY

1) S.A.E. Aerospace Material Specification 4976D, Society of Automotive Engineers, Warrendale PA, 1988.

2) W. Evans, and G. Harrison: *J. of Mat. Sci.*, 1983, vol. 18, pp. 3449-3455.

3) N. Paton and M. Mahoney: *Metall. Trans. A*, 1976, vol. 7A, pp. 1685-1694.

4) W. Cho, J.W. Jones, J.E. Allison and W.T. Donlon: *Proceedings of the Sixth International Titanium Conference*, France, 1988, pp.187-192.

5) P. J. Bania, J. A. Hall: *Proceedings of the Fifth International Titanium Conference*, Munich, 1984, pp. 2371-2378.

6) S. Ankem and S.R. Seagle: *Proceedings of the Fifth International Titanium Conference*, Munich., 1984, pp. 2411-2418.

7) S. R. Seagle, G.S. Hall and H.B. Bomberger: *Metals Engineering Quarterly*, Feb. 1972,
pp. 48-54

8) C. C. Chen, J. E. Coyne: *Titanium 80 Science and Technology* , TMS-AIME, 1980, pp. 1197-1207.

9) P.J. Bania, J. Hall, and L. Bidwell: *Interim Technical Report, AFML Contract #F33615-75-C-5089*, 1975.

10) C. Quesne, C. Duong, F.Charpentier, J. Fries and P. Lacombe: *J. of Less Common Metals*, 1979, vol. 68, pp. 133-142.

11) D. Hiatt and B. Bristow: OREMET Corp., Albany OR, Private Communication, 1991.

12) ASTM Testing Standard E696, *Annual Book of ASTM Standards*,. 3.1, Philadelphia PA, 1980, pg. 609.

13) C.W. Schmidt: *G.E Quality Specification S-400B*, Evendale OH, 1990, pp 24-26.

14) U. Kansal, M.E. Kassner, D. Hiatt, and B. Bristow: *J. Eng. Mater. and Perf.*, 1992, vol. 1, pp. 393-398.

15) M.E. Kassner and X. Li, *Scripta Met. et. Mater.* , 1991, vol. 25, pp. 2833-2838.

16) S. L. Semiatin, G. D. Lahoti: *Metall.Trans. A*, 1983, 14A, pp. 743-750.

17) O. D. Sherby, P. M. Burke: *Prog. in Mat. Sci.*, 1968, vol. 13, pp. 325-390.

APPENDIX

Figure 12. Creep Strain as a Function of Time for Ti 6242Si Samples Solution Annealed at Tß-52°C

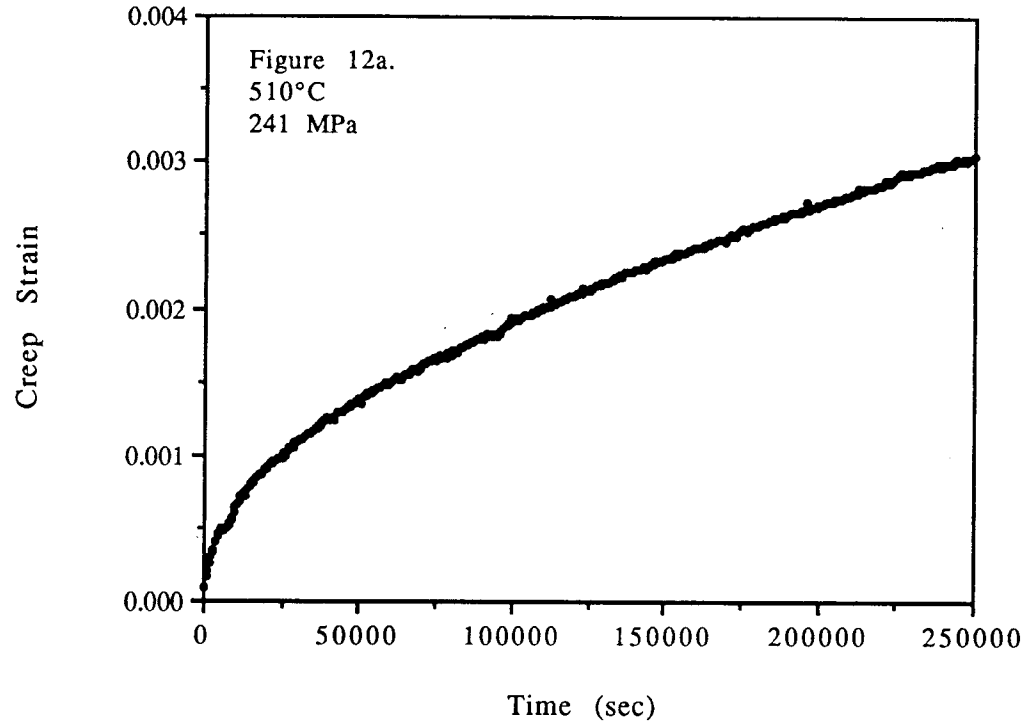

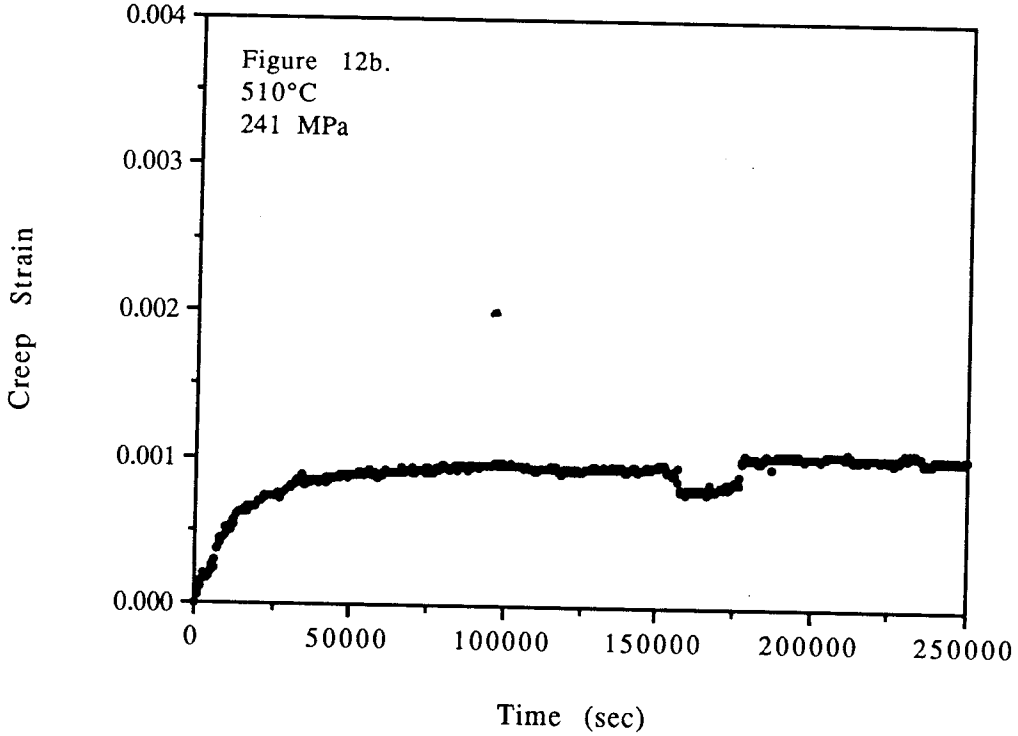

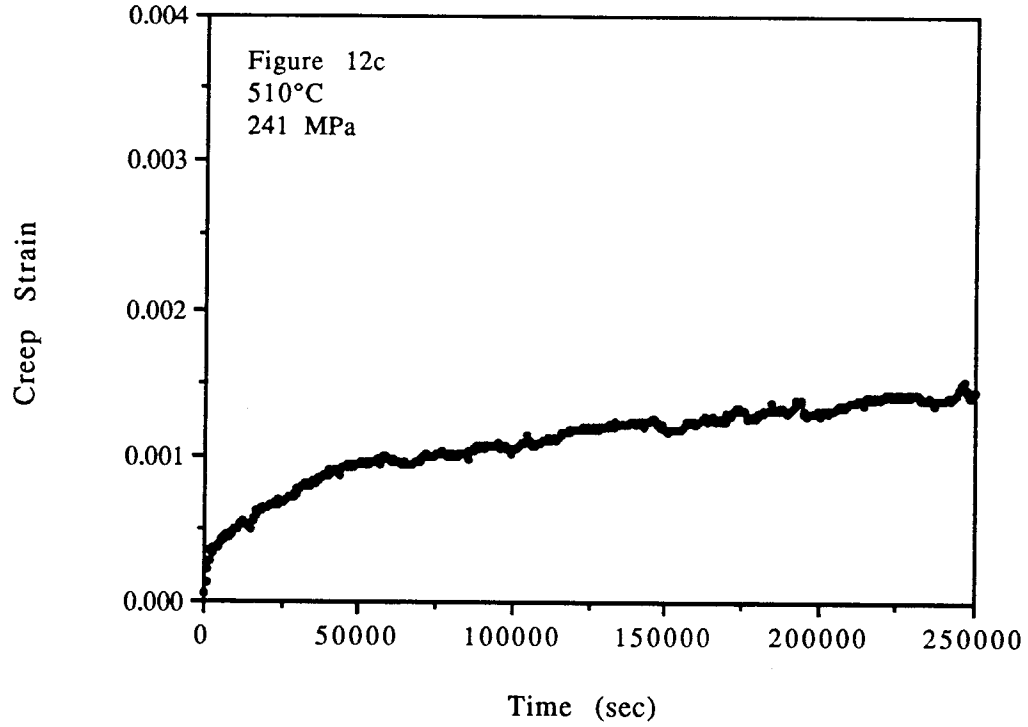
Figure 12c
510°C
241 MPa
Creep Strain
0.004
0.003
0.002
0.001
0.000
0
50000
100000
150000
200000
250000
Time (sec)

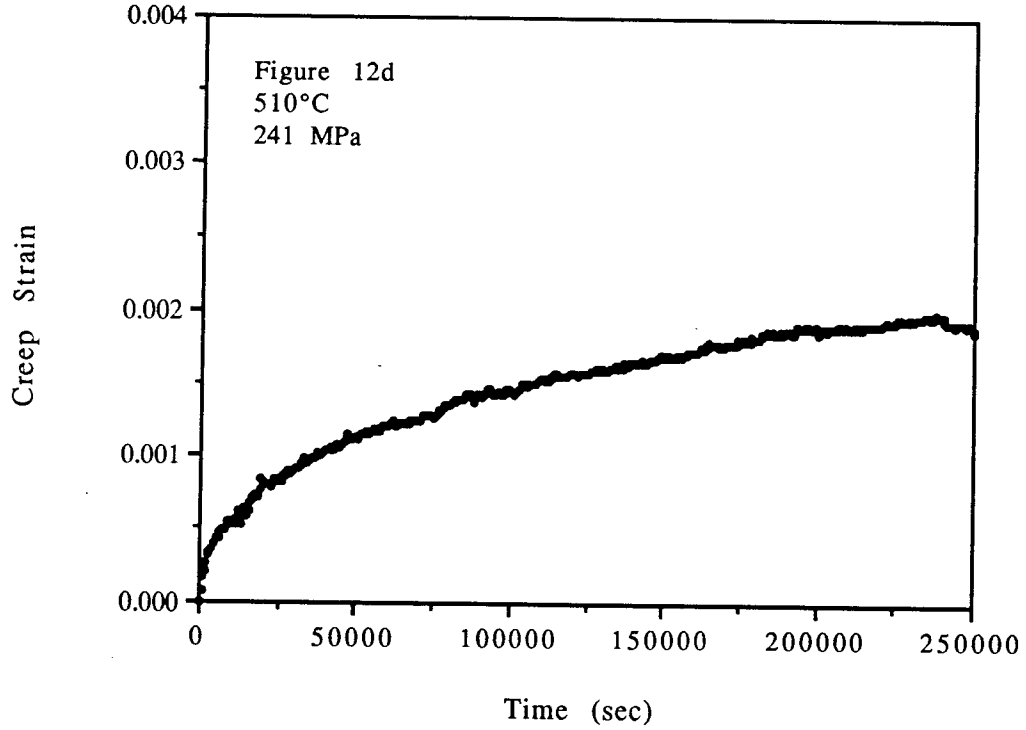
Figure 12d
510°C
241 MPa
Creep Strain
0.004
0.003
0.002
0.001
0.000
0
50000
100000
150000
200000
250000
Time (sec)

Figure 13. Creep Strain as a Function of Time for Ti 6242Si Samples Solution Annealed at Tß-28°C

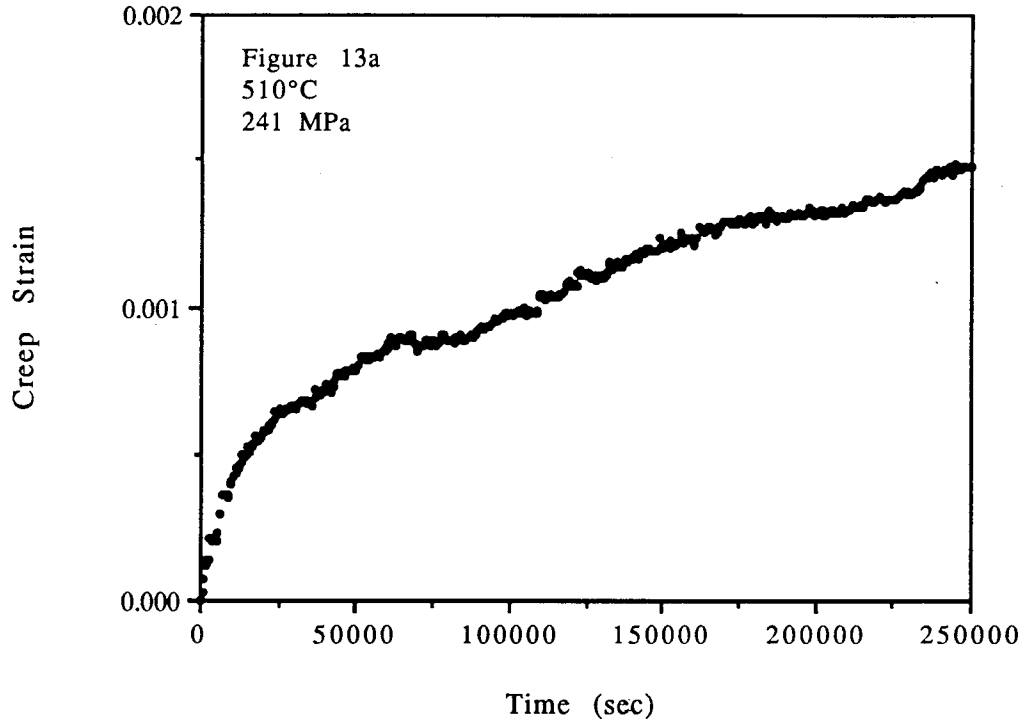

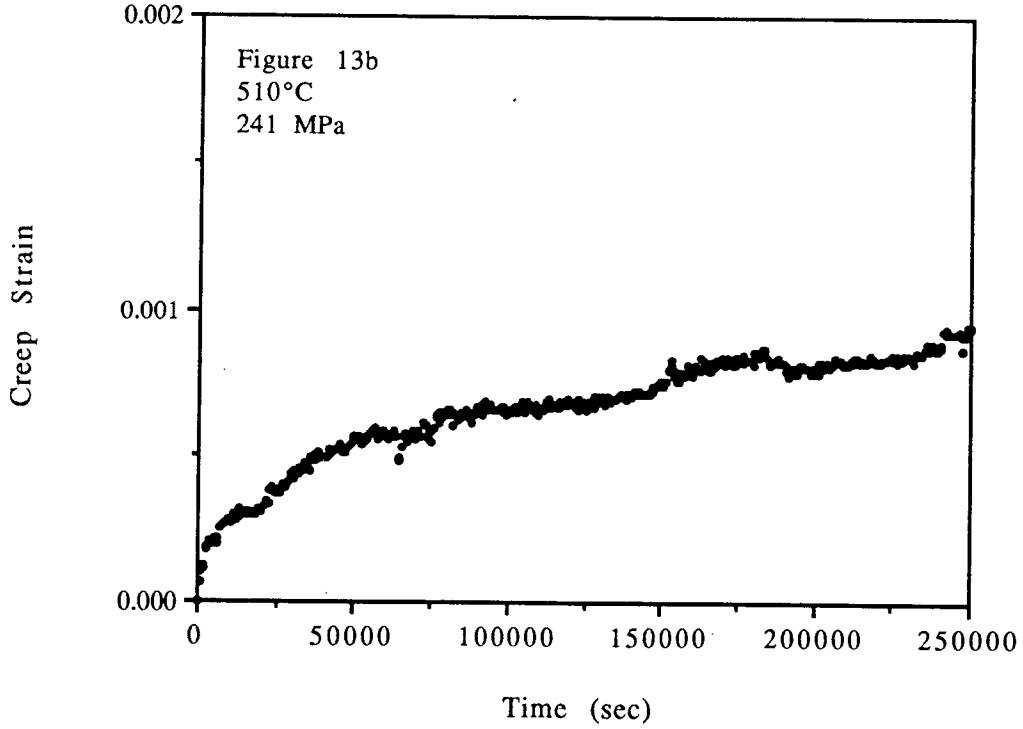

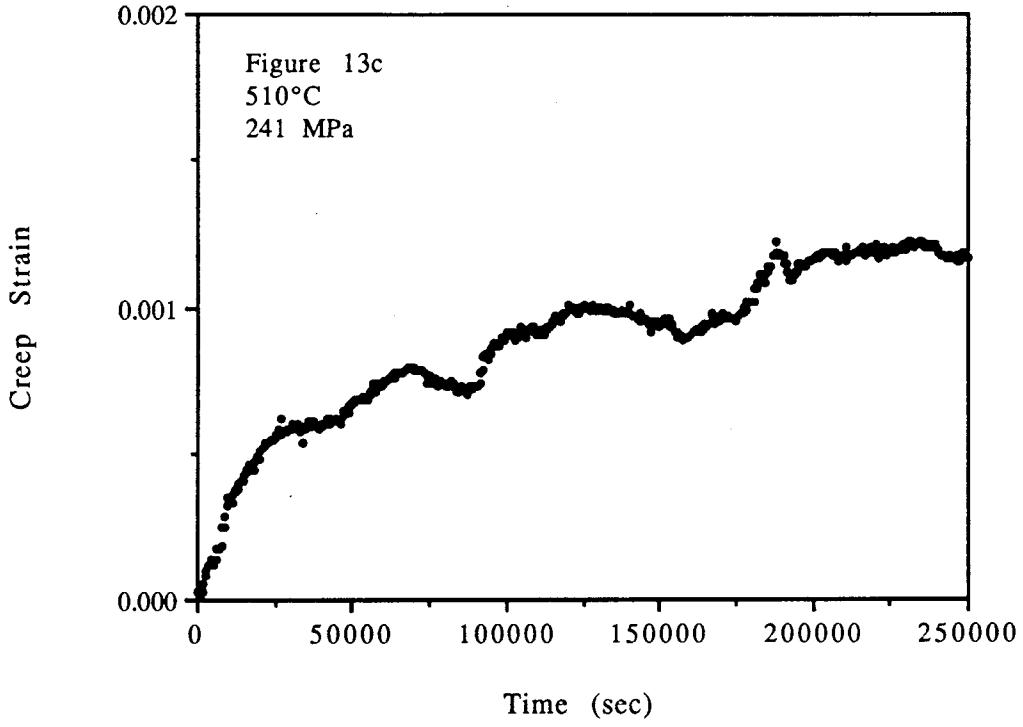
Figure 13c
510°C
241 MPa
Creep Strain
0.002
0.001
0.000
0
50000
100000
150000
200000
250000
Time (sec)

Figure 14. Creep Strain as a Function of Time for Ti 6242Si Samples Solution Annealed at Tß-15°C

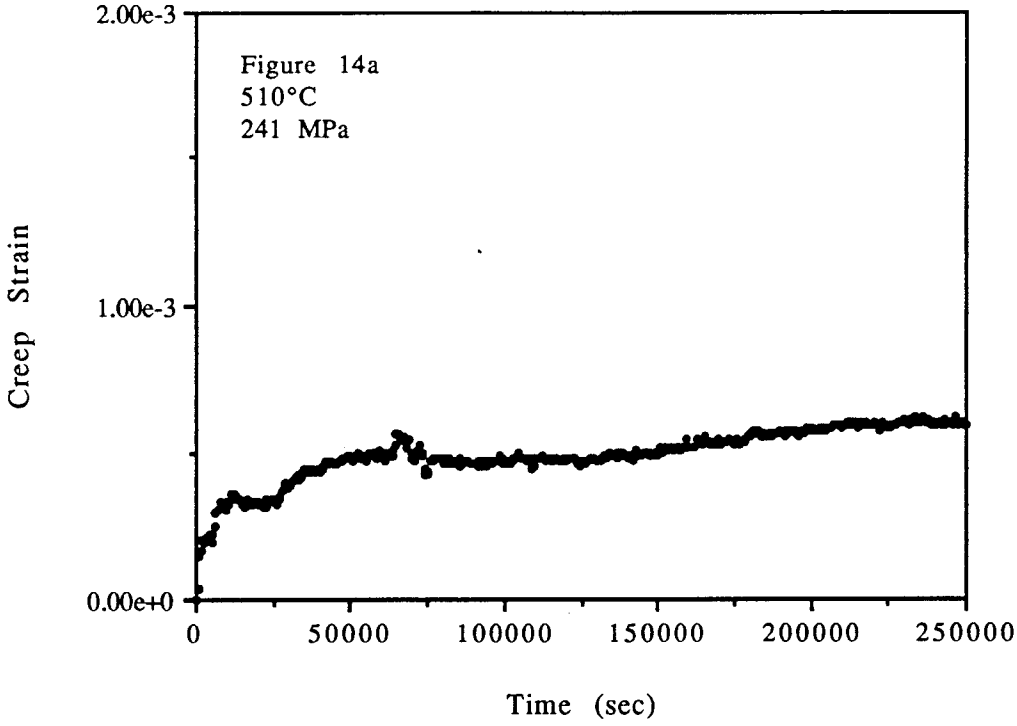

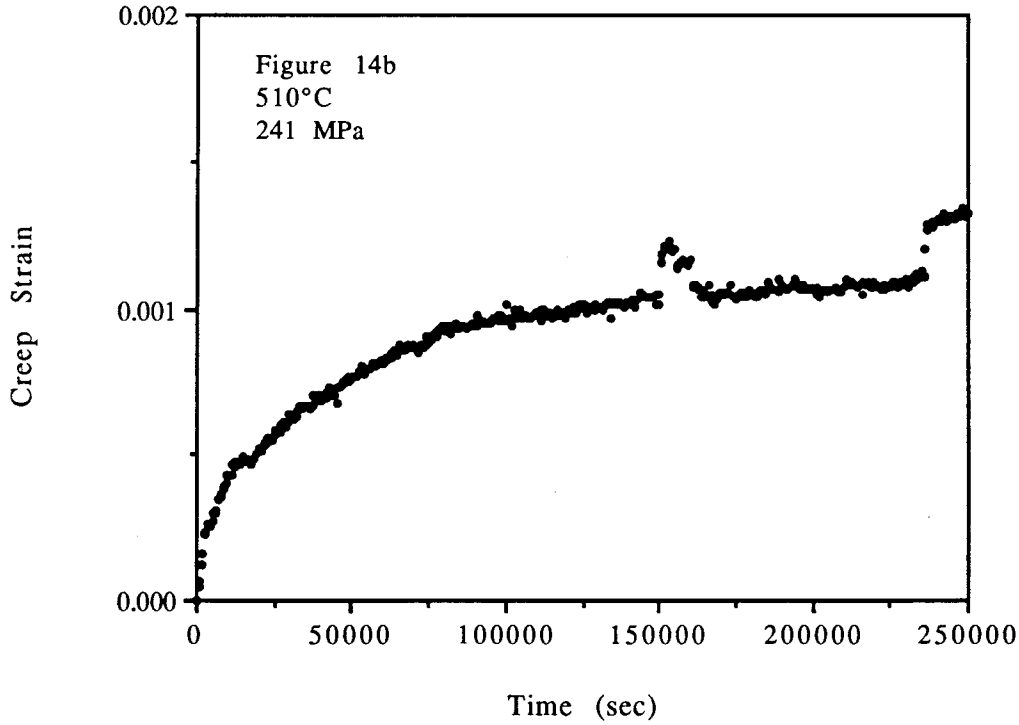

Figure 15. Creep Strain as a Function of Time for Ti 6242Si Samples Solution Annealed at Tß-6°C

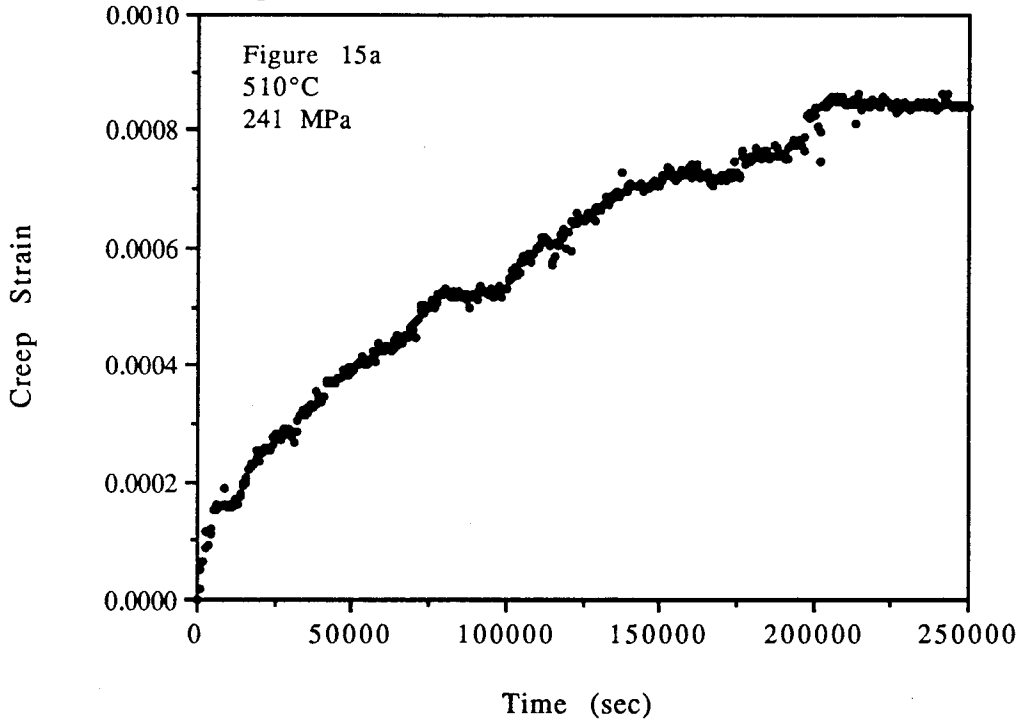

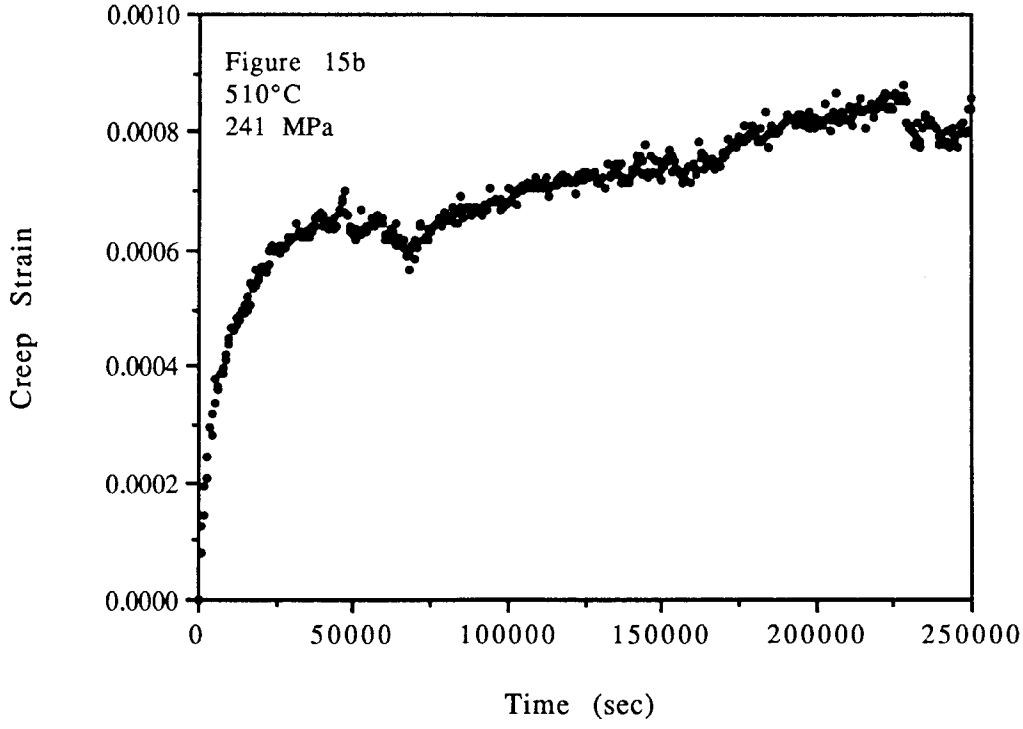

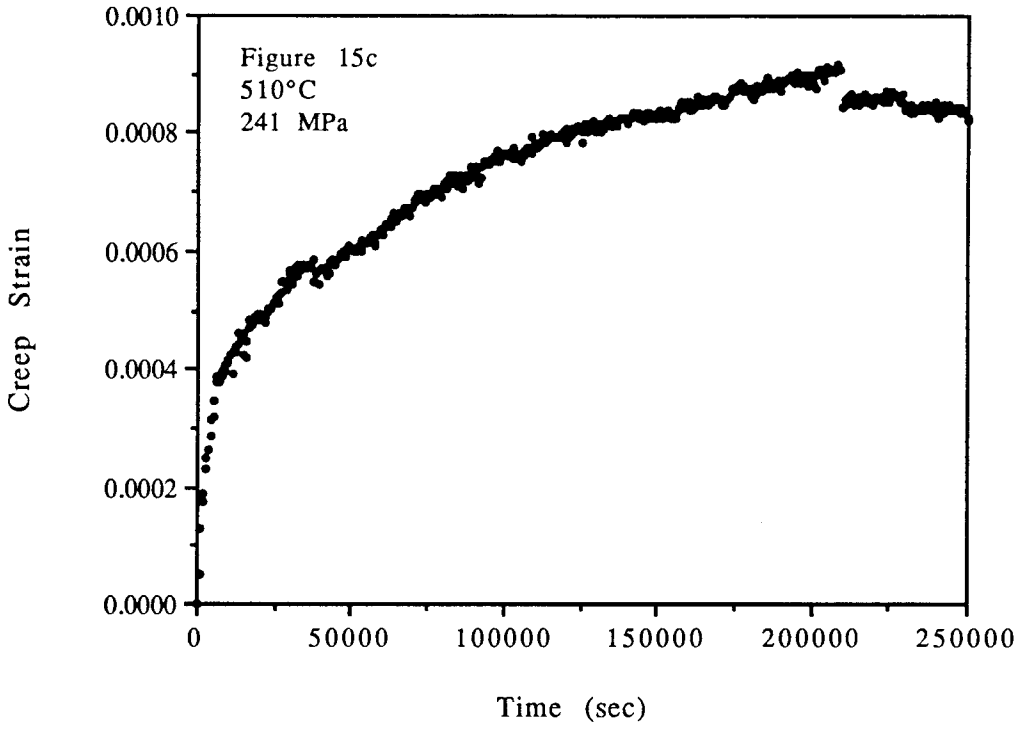
Figure 15c
510°C
241 MPa
Creep Strain
0.0010
0.0008
0.0006
0.0004
0.0002
0.0000
0
50000
100000
150000
200000
250000
Time (sec)

Figure 16. Creep Strain as a Fuction of Time for Ti 6242Si With No Impurity Additions

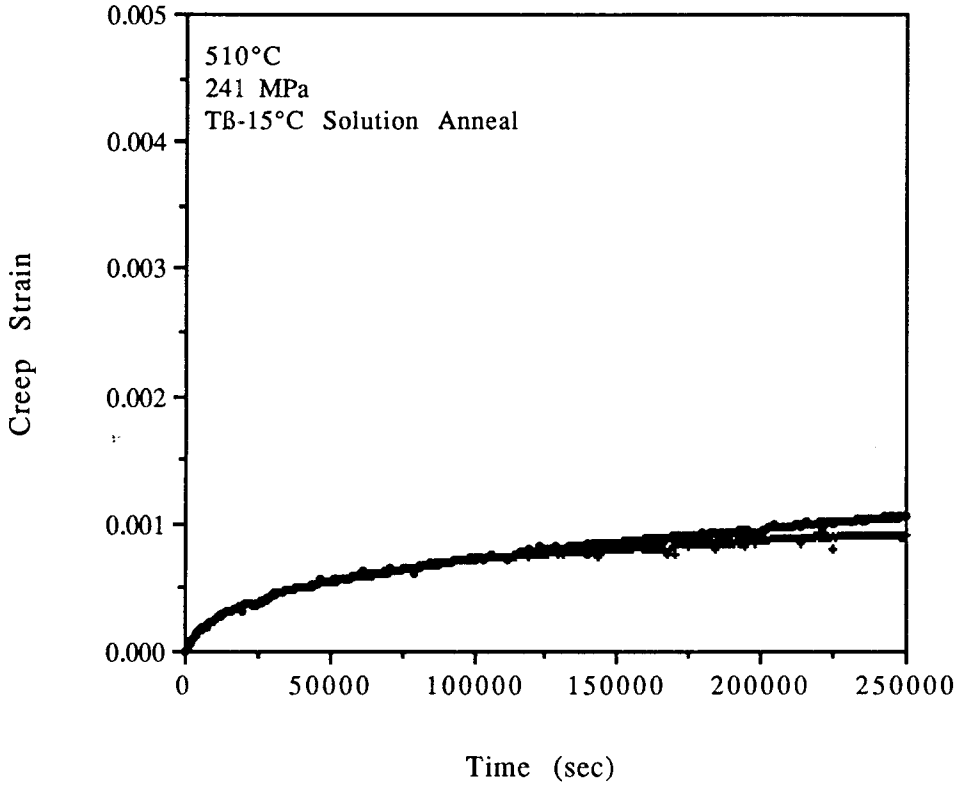

Figure 17. Creep Strain as a Function of Time for Ti 6242Si With 0.075wt% Added Ni

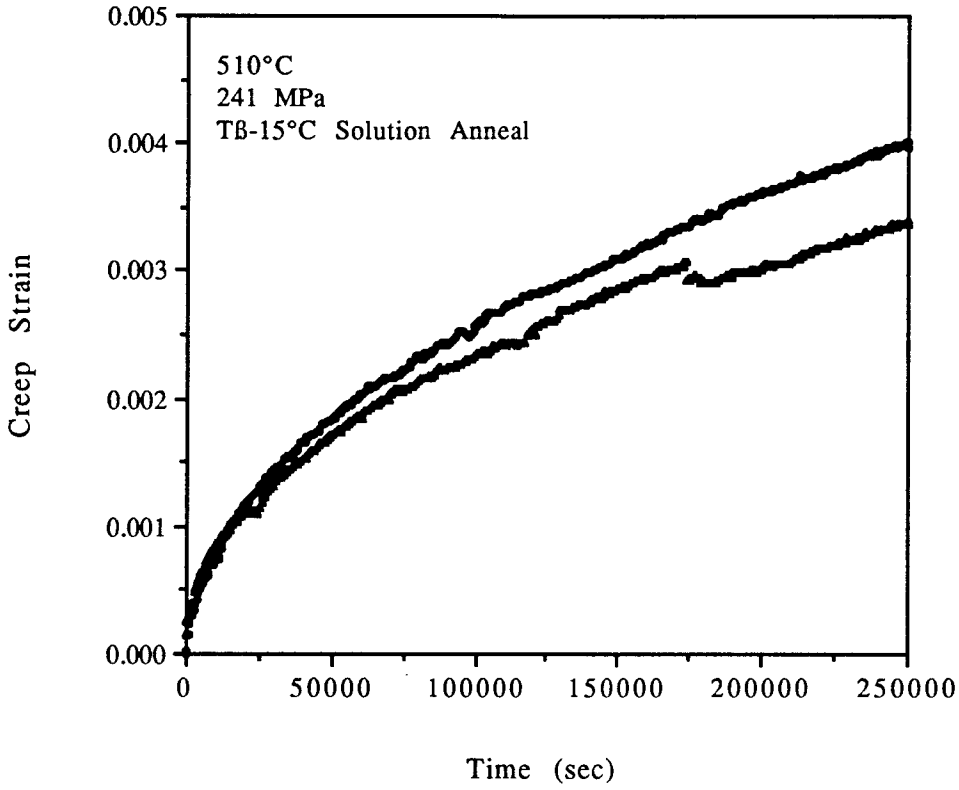

Figure 18. Creep Strain as a Function of Time for Ti 6242Si With 0.093wt% Added Ni

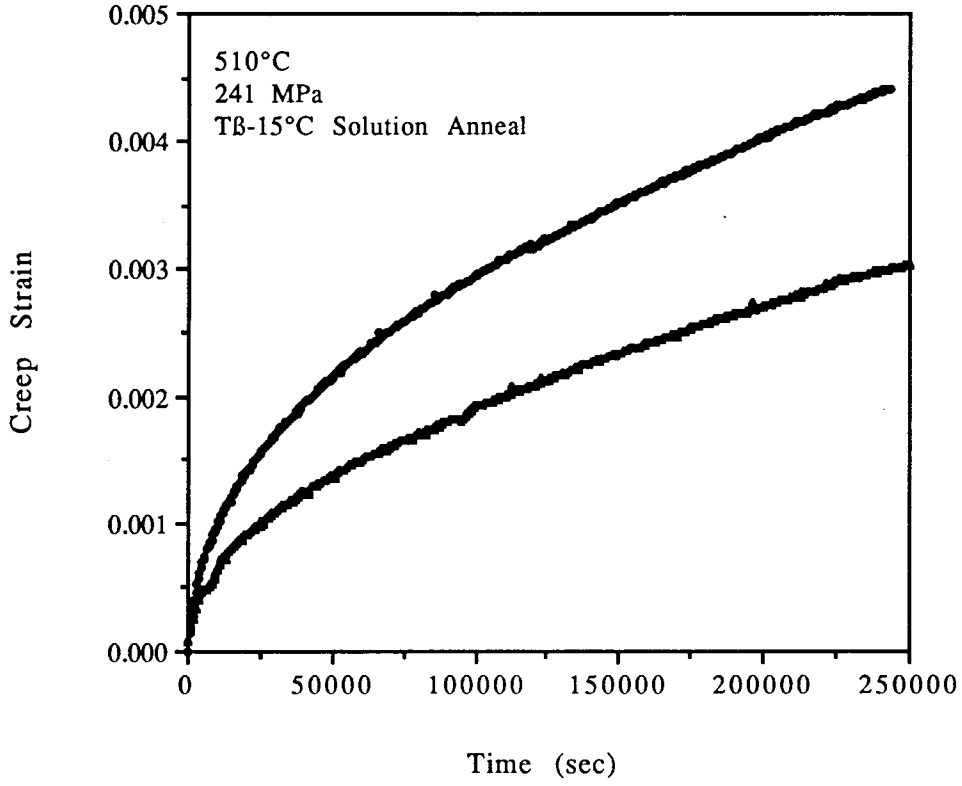

Figure 19. Creep Strain as a Function of Time for Ti 6242Si With 0.071wt% Added Cr

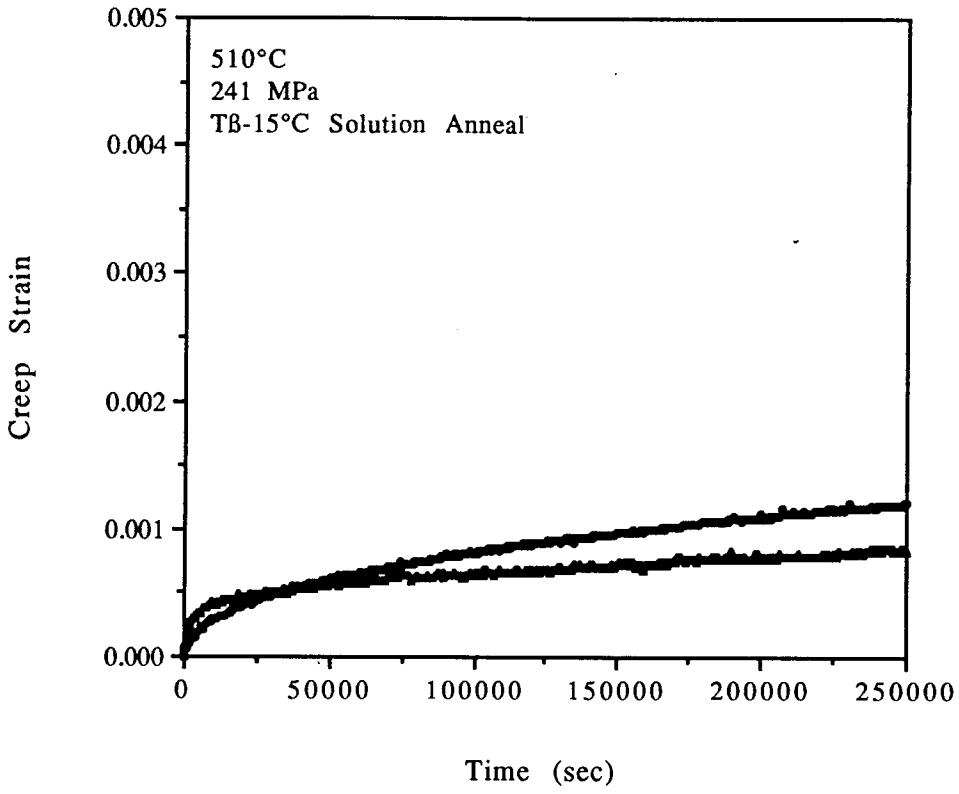

Figure 20. Creep Strain as a Function of Time for Ti 6242Si With 0.278wt% Added Cr

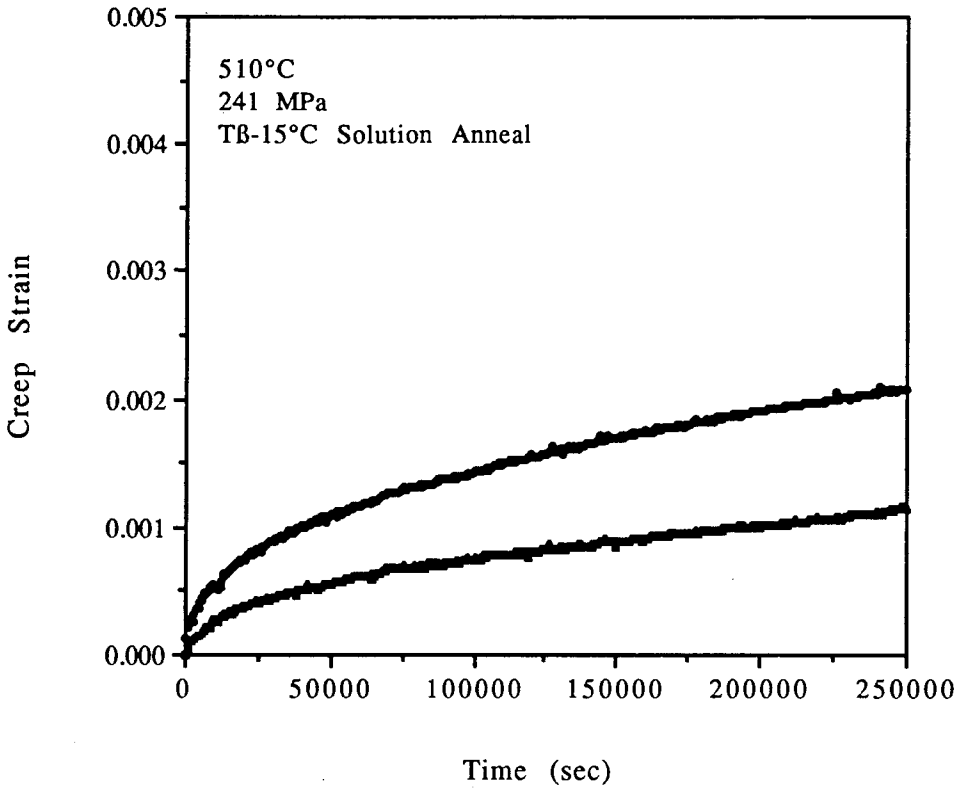

Figure 21. Typical Sample Temperature Variation During Creep Testing (taken during 0.278wt% Cr test)

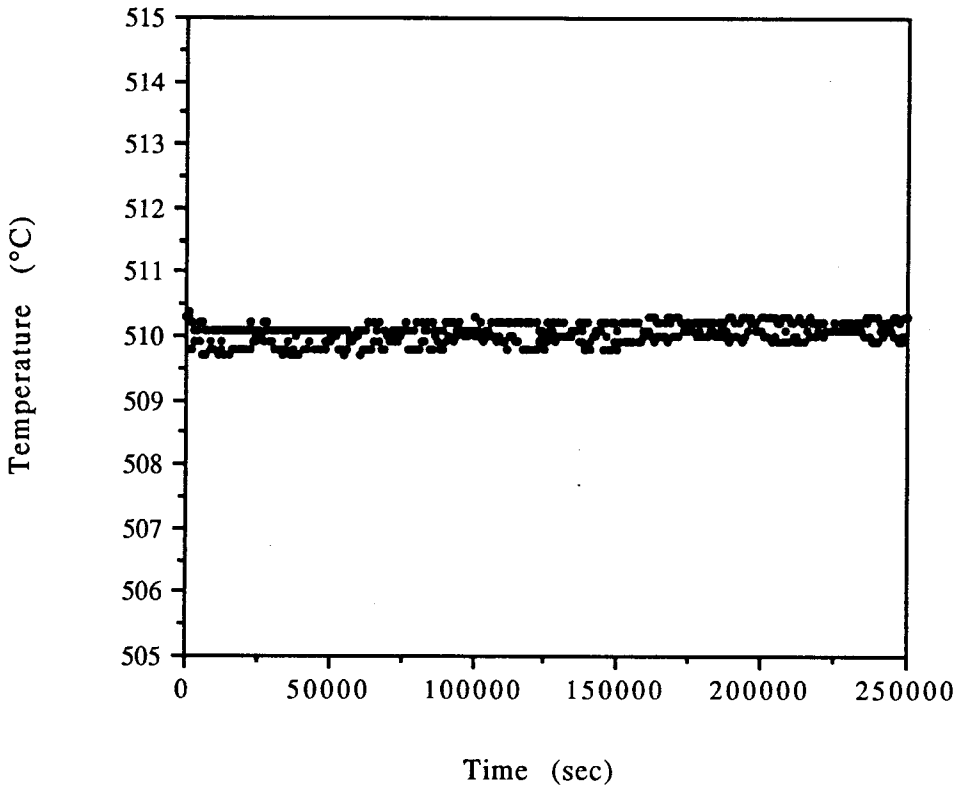

Figure 22a. α phase composition

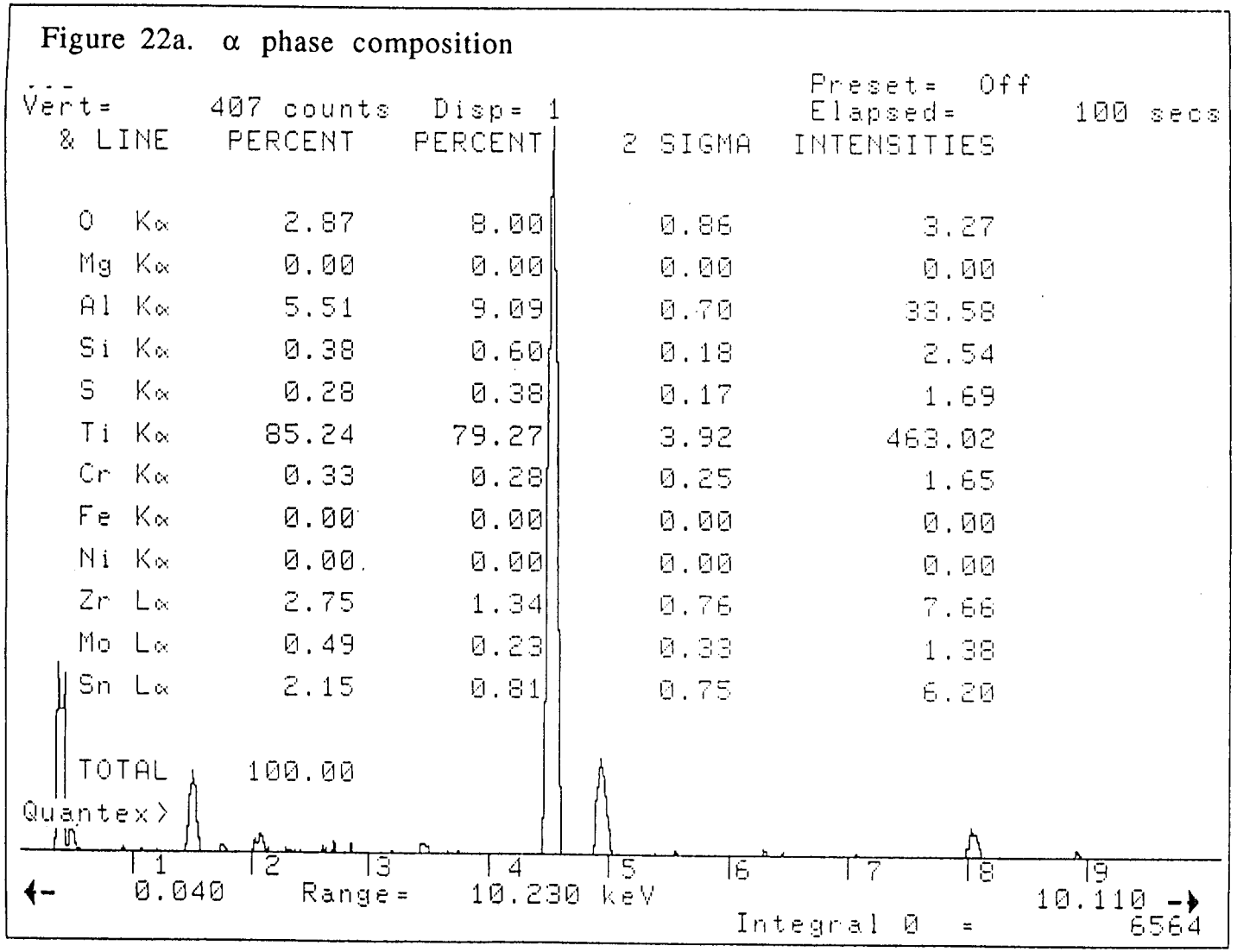

Figure 22. Raw XEDS report on composition of Ti 6242Si phases.

Figure 22b. Interfacial α phase composition

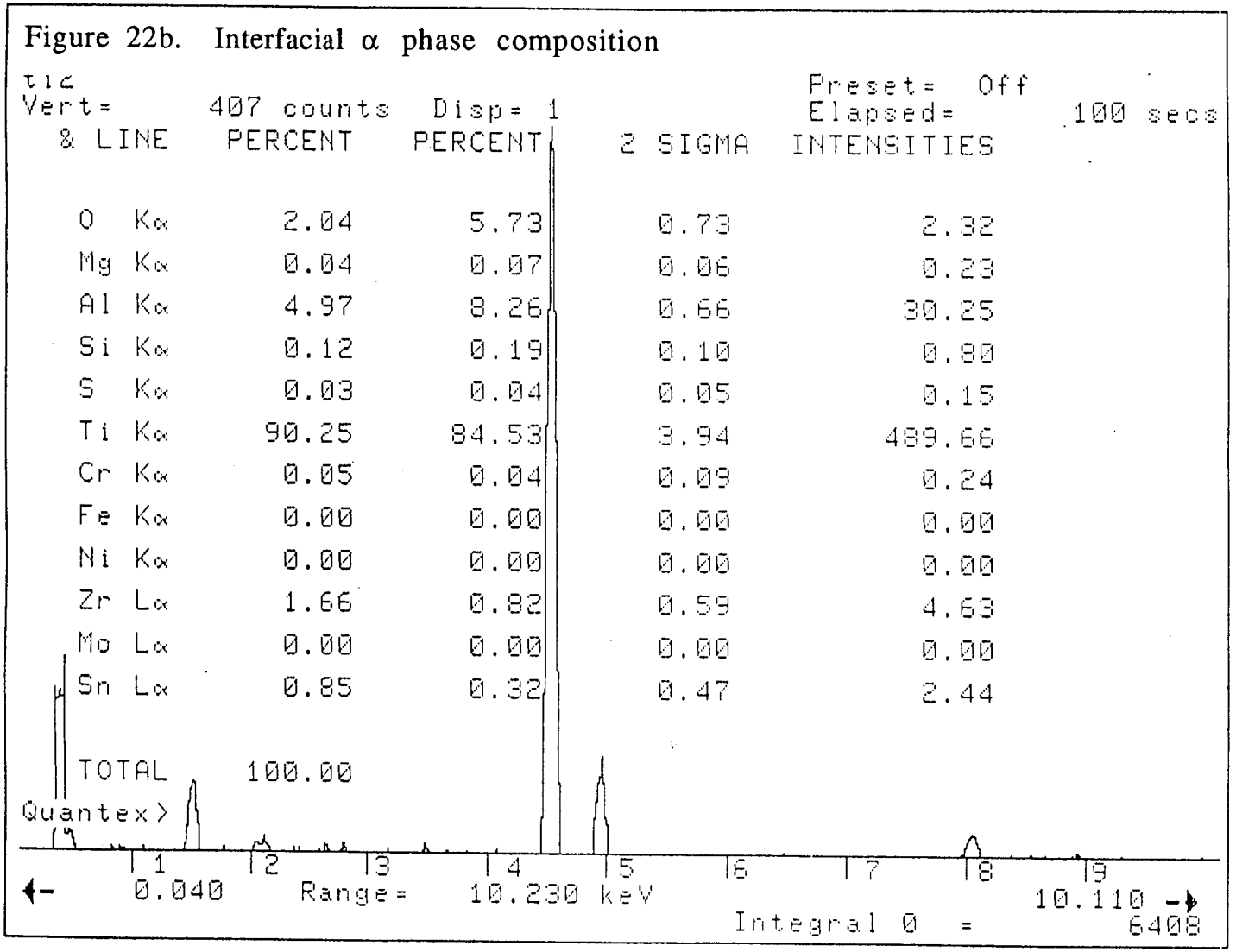

Figure 22c. β phase composition